

# **SAND REPORT**

SAND2002-1882  
Unlimited Release  
Printed July 2002

## **ELASTIC WAVE RADIATION FROM A PRESSURIZED SPHERICAL CAVITY**

David F. Aldridge

Prepared by  
Sandia National Laboratories  
Albuquerque, New Mexico 87185 and Livermore, California 94550

Sandia is a multiprogram laboratory operated by Sandia Corporation,  
a Lockheed Martin Company, for the United States Department of  
Energy under Contract DE-AC04-94AL85000.

Approved for public release; further dissemination unlimited.



**Sandia National Laboratories**

Issued by Sandia National Laboratories, operated for the United States  
Department of Energy by Sandia Corporation.

**NOTICE:** This report was prepared as an account of work sponsored by an agency of the United States Government. Neither the United States Government, nor any agency thereof, nor any of their employees, nor any of their contractors, subcontractors, or their employees, make any warranty, express or implied, or assume any legal liability or responsibility for the accuracy, completeness, or usefulness of any information, apparatus, product, or process disclosed, or represent that its use would not infringe privately owned rights. Reference herein to any specific commercial product, process, or service by trade name, trademark, manufacturer, or otherwise, does not necessarily constitute or imply its endorsement, recommendation, or favoring by the United States Government, any agency thereof, or any of their contractors or subcontractors. The views and opinions expressed herein do not necessarily state or reflect those of the United States Government, any agency thereof, or any of their contractors.

Printed in the United States of America. This report has been reproduced directly from the best available copy.

Available to DOE and DOE contractors from  
U.S. Department of Energy  
Office of Scientific and Technical Information  
P.O. Box 62  
Oak Ridge, TN 37831

Telephone: (865)576-8401  
Facsimile: (865)576-5728  
E-Mail: [reports@adonis.osti.gov](mailto:reports@adonis.osti.gov)  
Online ordering: <http://www.doe.gov/bridge>

Available to the public from  
U.S. Department of Commerce  
National Technical Information Service  
5285 Port Royal Rd  
Springfield, VA 22161

Telephone: (800)553-6847  
Facsimile: (703)605-6900  
E-Mail: [orders@ntis.fedworld.gov](mailto:orders@ntis.fedworld.gov)  
Online order: <http://www.ntis.gov/ordering.htm>



SAND2002-1882  
Unlimited Release  
Printed July 2002

## **ELASTIC WAVE RADIATION FROM A PRESSURIZED SPHERICAL CAVITY**

David F. Aldridge  
Geophysical Technology Department  
Sandia National Laboratories  
P.O. Box 5800  
Albuquerque, New Mexico, USA, 87185-0750

### **ABSTRACT**

Elastic waves radiated from a pressurized spherical cavity embedded within a homogeneous and isotropic wholespace are described by closed-form mathematical formulae, in both the time-domain and the frequency-domain. For this spherically symmetric problem, only radially polarized compressional waves are generated. All near-field and far-field terms are included in the solution, and the expressions are valid for arbitrary source pressure waveforms. Analogous formulae are developed for the elastic wavefield produced by a uniform radial particle displacement imposed at the cavity wall. These closed-form mathematical solutions facilitate rapid and accurate forward modeling, and hence are particularly useful for (i) performing order-of-magnitude estimations of various cavity-source elastic radiation phenomena, and (ii) validating purely numerical (i.e., finite-element or finite-difference) algorithms designed to solve similar problems. The formulae also indicate that the inverse source characterization problem is well posed: the source activation wavelet (pressure, traction, displacement, velocity, etc.) is obtained by performing a deterministic deconvolution of the response observed at a remote receiver. Numerical examples verify that the source signature is accurately recovered, provided the elastic parameters, recording geometry, and cavity radius are known.

## **ACKNOWLEDGEMENTS**

Sandia National Laboratories is a multiprogram science and engineering facility operated by Sandia Corporation, a Lockheed-Martin company, for the United States Department of Energy under contract DE-AC04-94AL85000.

This research is undertaken in support of Laboratory Directed Research and Development (LDRD) project entitled "Use of seismic and acoustic responses to assess bomb damage to underground facilities" (Principal Investigator: Dr. Lewis C. Bartel, Geophysical Technology Department, Sandia National Laboratories, Albuquerque, New Mexico, 87185-0750).

Aspects of this research were initiated when the author was a geophysicist with Chevron Oil Field Research Company / Chevron Petroleum Technology Company, 1300 Beach Boulevard, La Habra, California, 90631-6374, during the period 1992-1995.

# CONTENTS

<b>1.0 Introduction</b> .....	1
<b>2.0 Spherically Symmetric Source</b> .....	2
<b>3.0 Field Equations</b> .....	3
<b>4.0 General Solution</b> .....	3
<b>5.0 Radiation and Boundary Conditions</b> .....	5
<b>6.0 Frequency-Domain Solution</b> .....	6
<b>7.0 Time-Domain Solution</b> .....	7
<b>8.0 Examples and Applications</b> .....	9
8.1 Static Loading	
8.2 Explosive Loading	
8.3 Acoustic Medium	
8.4 Far-Field Approximation	
8.5 Point Source	
8.6 Scaling Relations	
<b>9.0 Radiated Energy</b> .....	12
9.1 Explosive Loading	
9.2 Energy Scaling	
<b>10.0 Inverse Impulse Response</b> .....	16
<b>11.0 ART Representation</b> .....	17
<b>12.0 Displacement Boundary Condition</b> .....	19
12.1 Frequency-Domain Solution	
12.2 Time-Domain Solution	
12.3 Static, Step, and Exponential Displacements	
12.4 Point Source	
12.5 Scaling Relations	
12.6 Radiated Energy	
12.7 Inverse Impulse Response	
12.8 ART Representation	
<b>13.0 Numerical Examples</b> .....	24
<b>14.0 Conclusion</b> .....	26
<b>15.0 References</b> .....	27
<b>16.0 Figures</b> .....	29

## 1.0 INTRODUCTION

When an explosive seismic energy source is detonated within a solid or fluid continuum, a zone of nonlinear deformation is produced in the immediate vicinity of the explosion. As the shock wavefront propagates outward through this zone, it rapidly loses amplitude due to irreversible conversion of wave energy to heat, as well as geometric divergence. Eventually, a radius is reached where material deformations, strains, and stresses have decayed to a level sufficient for linear wave propagation theories to apply. If the outgoing wavefield is known on the spherical surface with this particular radius, then relatively straightforward mathematical and/or numerical procedures developed from these linear theories may be used to calculate the wavefield at greater distances.

In the simple situation where the continuum surrounding the explosion is taken to be a homogeneous and isotropic elastic wholespace, the radiated wavefield is characterized by closed-form mathematical formulae. Perhaps Jeffreys (1931) was the first to obtain the solution for compressional (P-wave) elastic radiation from a small spherical cavity subject to an instantaneous step in internal pressure. Numerous investigators (many referenced herein) have refined and extended this solution. The pressurized cavity source has subsequently been utilized to simulate and analyze seismic data arising in a variety of geophysical contexts, e.g. earthquake seismology, mine blasting, underground nuclear explosions, and petroleum exploration.

In the present study, the spherically symmetric cavity source problem is re-examined, and several improvements to the solution are developed. Specifically, these improvements include:

- 1) The source activation wavelet  $s(t)$  is considered an arbitrary function of time. Many previous investigators have restricted this waveform to specific mathematical forms, like the instantaneously-applied and infinitely-maintained step in cavity pressure  $s(t) = s_0 H(t)$  (where  $H(t)$  is the Heaviside unit step function). The resulting formulae for the radiated compressional waves are similarly restricted in applicability.
- 2) The boundary condition applied at the spherical cavity wall is generalized to include a prescribed radial particle displacement function. All previous investigators have utilized a radial stress function at the spherical interface. Complicated physical and continuum mechanical processes occur adjacent to an explosion seismic source. Hence, it is not obvious what boundary condition should be imposed at the surface separating zones of nonlinear and linear deformation. The new formulae derived for the displacement boundary condition provide an additional degree of flexibility for modeling elastic wavefields generated by explosive sources. Interestingly, these expressions have a very different mathematical character than the analogous formulae for an applied radial stress. Also, they are simpler.
- 3) Expressions for the total elastic energy (sum of kinetic energy and strain energy) radiated from the cavity are developed, for both types of source boundary conditions and for a general source activation wavelet. These energy expressions may be useful for explosion yield estimation.
- 4) The inverse problem associated with determining the source signature is developed, again for both types of boundary conditions and for a general source activation wavelet. Expressions for the elastic response (particle displacement, velocity, acceleration, or pressure) at a remote receiver are readily inverted (via either time-domain or frequency-domain methods) to obtain the source waveform applied to the spherical cavity wall. The particular mathematical procedure corresponds to a deterministic deconvolution of the recorded traces. Accurate recovery of the source waveform requires knowledge of the source-receiver geometry, the cavity radius, and the elastic parameters of the wholespace. Interestingly, it is *not* necessary to know the particular type of boundary condition imposed at the cavity

wall (radial stress, displacement, velocity, acceleration, etc.), in order to perform a useful source signature deconvolution.

The particular motivation for undertaking this re-examination of the cavity source elastic radiation problem is to assess the feasibility of using observed seismic data to determine the pressure generated by a bomb explosion. In this scenario, seismic receivers will be distributed relatively close to the bomb detonation point, so the assumption of a homogeneous and isotropic elastic wholespace for the analysis may not be unduly restrictive. Moreover, the source signature deconvolution process may be effective if it is applied to the initial compressional arrival observed at each receiver, and subsequent reflected, refracted, scattered, surface wave, etc. arrivals are neglected. Close proximity of the receivers to the explosion point requires that all near-field terms be included in the mathematical formulae used for both forward modeling and inversion.

Finally, several numerical examples illustrate the utility of the derived formulae for both forward modeling and source signature inversion purposes.

## 2.0 SPHERICALLY SYMMETRIC SOURCE

Consider a spherical cavity of radius  $a$  embedded in a homogeneous and isotropic elastic wholespace. A uniform, time-varying normal stress  $s(t)$  is applied to the interior surface of the cavity. Spherically diverging waves are generated that propagate outward from the cavity wall with the compressional wave speed of the medium. The problem is to determine the elastic particle displacement at a field point P with position vector  $\mathbf{r}$ .

A spherical polar coordinate system with origin at the cavity center is used in the subsequent analysis. From symmetry considerations, the elastic particle displacement vector  $\mathbf{u}(\mathbf{r},t)$  is strictly radial and is independent of the two angular coordinates  $\theta$  and  $\phi$ . Thus:

$$\mathbf{u}(\mathbf{r},t) = u(r,t) \mathbf{e}_r, \quad (2.1)$$

where  $\mathbf{e}_r$  is a unit radial vector for the spherical polar coordinate system.

A graphic depiction of the problem geometry is given in figure 1. In general, the boundary condition imposed at the spherical interface  $r = a$  may consist of a prescribed radial displacement, velocity, acceleration, or traction function (or any linear combination thereof). This boundary condition must be uniform (i.e., spatially invariant) in order to preserve the spherically symmetric nature of the problem. The equivalent elastic radius concept is illustrated in figure 2. The spherical surface with radius  $a$  is now considered a reference surface, rather than a physical interface, separating zones of nonlinear deformation (for  $r < a$ ) and linear elastic deformation (for  $r > a$ ). Of course, *any* spherical surface with radius larger than  $a$  could be utilized as the reference surface. The only requirement is that linear elasticity apply at all greater radial distances.

The mathematical development in the sections that immediately follow pertains to the more difficult case where the boundary condition at  $r = a$  is a prescribed radial stress function. A later section treats the simpler radial displacement boundary condition. The formulae pertaining to the displacement boundary condition are readily generalized to particle velocity or particle acceleration boundary conditions, merely by differentiating (in the time-domain) or by multiplying by a power of frequency (in the spectral-domain).

### 3.0 FIELD EQUATIONS

The elastic particle displacement vector  $\mathbf{u}(\mathbf{r},t)$  satisfies the elastodynamic equation. For the case of a homogeneous and isotropic solid subject to no body forces or body moments, this is

$$(\lambda + \mu) \mathbf{grad} \operatorname{div} \mathbf{u} + \mu \nabla^2 \mathbf{u} = \rho \frac{\partial^2 \mathbf{u}}{\partial t^2}, \quad (3.1)$$

where  $\lambda$  and  $\mu$  are the Lamé coefficients and  $\rho$  is the mass density. An alternate form is obtained by using the identity  $\nabla^2 \mathbf{u} = \mathbf{grad} \operatorname{div} \mathbf{u} - \mathbf{curl} \operatorname{curl} \mathbf{u}$ . Thus

$$(\lambda + 2\mu) \nabla^2 \mathbf{u} + (\lambda + \mu) \mathbf{curl} \operatorname{curl} \mathbf{u} = \rho \frac{\partial^2 \mathbf{u}}{\partial t^2}. \quad (3.2)$$

The particular displacement under consideration [equation (2.1)] is curl-free motion; that is  $\mathbf{curl} \mathbf{u}(\mathbf{r},t) = \mathbf{curl} [u(r,t) \mathbf{e}_r] = \mathbf{0}$ . Hence, expression (3.2) reduces to

$$\nabla^2 \mathbf{u} - \frac{1}{\alpha^2} \frac{\partial^2 \mathbf{u}}{\partial t^2} = \mathbf{0}, \quad (3.3)$$

where  $\alpha = \sqrt{(\lambda + 2\mu)/\rho}$  is the compressional wave speed of the elastic medium. Expression (3.3) indicates that a curl-free displacement  $\mathbf{u}(\mathbf{r},t)$  satisfies the three-dimensional vector wave equation.

### 4.0 GENERAL SOLUTION

Under the aforementioned conditions of spherical symmetry, the Laplacian of the vector  $\mathbf{u}$  is

$$\nabla^2 \mathbf{u} = \left[ \frac{\partial^2 u}{\partial r^2} + \frac{2}{r} \frac{\partial u}{\partial r} - \frac{2u}{r^2} \right] \mathbf{e}_r. \quad (4.1)$$

Thus, the radial component of the wave equation (3.3) is

$$\frac{\partial^2 u}{\partial r^2} + \frac{2}{r} \frac{\partial u}{\partial r} - \frac{2u}{r^2} - \frac{1}{\alpha^2} \frac{\partial^2 u}{\partial t^2} = 0. \quad (4.2)$$

Equation (4.2) can be solved after removing the time dependence by Fourier transformation. The Fourier transform of the radial displacement component  $u(r,t)$  is defined by

$$U(r, f) = \int_{-\infty}^{+\infty} u(r, t) e^{-i2\pi ft} dt. \quad (4.3)$$

Hence, Fourier transforming equation (4.2) gives

$$\frac{\partial^2 U}{\partial r^2} + \frac{2}{r} \frac{\partial U}{\partial r} + \left[ \left( \frac{2\pi f}{\alpha} \right)^2 - \frac{2}{r^2} \right] U = 0, \quad (4.4)$$

where the derivative theorem of Fourier transformation is used.

Equation (4.4) can be transformed to Bessel's equation by an appropriate change of variables. First, define a new independent variable  $x$  via  $x \equiv kr$  where  $k = 2\pi f / \alpha$ . Then  $U(r, f) = U(x/k, f) \equiv V(x, f)$ . Equation (4.4) becomes

$$\frac{\partial^2 V}{\partial x^2} + \frac{2}{x} \frac{\partial V}{\partial x} + \left[ 1 - \frac{2}{x^2} \right] V = 0.$$

Now define a new dependent variable  $W(x, f) \equiv \sqrt{x} V(x, f)$ . The above expression reduces to

$$\frac{\partial^2 W}{\partial x^2} + \frac{1}{x} \frac{\partial W}{\partial x} + \left[ 1 - \frac{(3/2)^2}{x^2} \right] W = 0.$$

This is Bessel's differential equation of order  $3/2$ . It has the solution

$$W(x, f) = A J_{3/2}(x) + B N_{3/2}(x),$$

where  $J_{3/2}(x)$  and  $N_{3/2}(x)$  are the Bessel and Neumann functions of order  $3/2$ , respectively.  $A$  and  $B$  are coefficients that are independent of  $x$ , but may depend on frequency  $f$ . In terms of the original independent and dependent variables, the solution to (4.4) is

$$U(r, f) = A \frac{1}{\sqrt{kr}} J_{3/2}(kr) + B \frac{1}{\sqrt{kr}} N_{3/2}(kr). \quad (4.5)$$

The spherical Bessel and Neumann functions of order  $l$  are defined as

$$j_l(x) = \sqrt{\frac{\pi}{2}} \frac{1}{\sqrt{x}} J_{l+1/2}(x), \quad n_l(x) = \sqrt{\frac{\pi}{2}} \frac{1}{\sqrt{x}} N_{l+1/2}(x),$$

(Wylde, 1976, p. 178). Thus, equation (4.5) is written as

$$U(r, f) = A j_1(kr) + B n_1(kr), \quad (4.6)$$

where the factors  $\sqrt{(\pi/2)}$  are incorporated into the coefficients  $A$  and  $B$ . In turn, the spherical Bessel and Neumann functions can be expressed in terms of elementary trigonometric functions:

$$j_1(x) = -\frac{\cos x}{x} + \frac{\sin x}{x^2}, \quad n_1(x) = -\frac{\sin x}{x} - \frac{\cos x}{x^2}.$$

However, subsequent analysis is simplified if these functions are re-written in terms of complex exponentials. Substituting  $\cos x = [\exp(+ix) + \exp(-ix)]/2$  and  $\sin x = [\exp(+ix) - \exp(-ix)]/2i$  into the above expressions results in

$$j_1(x) = -\frac{1}{2}e^{+ix} \left[ \frac{1}{x} + \frac{i}{x^2} \right] - \frac{1}{2}e^{-ix} \left[ \frac{1}{x} - \frac{i}{x^2} \right], \quad n_1(x) = +\frac{1}{2}e^{+ix} \left[ \frac{i}{x} - \frac{1}{x^2} \right] - \frac{1}{2}e^{-ix} \left[ \frac{i}{x} + \frac{1}{x^2} \right].$$

Finally, substituting these expressions for the spherical Bessel and Neumann functions into equation (4.6) yields the following form for the Fourier transformed radial particle displacement:

$$U(r, f) = Ce^{+ikr} \left[ \frac{1}{kr} + \frac{i}{(kr)^2} \right] + De^{-ikr} \left[ \frac{1}{kr} - \frac{i}{(kr)^2} \right], \quad (4.7)$$

where  $C$  and  $D$  are coefficients that depend on the frequency  $f$ . It should be recalled that  $k$  also depends on frequency via  $k = 2\pi f / \alpha$ . Equation (4.7) is a general solution for the Fourier transformed radial particle displacement, under the specified conditions of spherical symmetry. The coefficients  $C$  and  $D$  are determined by introducing additional radiation and boundary conditions into the problem.

## 5.0 RADIATION AND BOUNDARY CONDITIONS

The first and second terms in the general solution (4.7) correspond to inward propagating and outward propagating spherical waves, respectively. This can be established by considering the kernel function for inverse Fourier transformation. Multiplying  $\exp(+ikr)$  in the first term by  $\exp(+i2\pi ft)$  gives  $\exp[i2\pi f(t+r/\alpha)]$ , which exhibits the proper time dependence for inward propagation. Similarly, the inverse Fourier transform of the second term in (4.7) has the time dependence  $t - r/\alpha$  appropriate for outward propagation. Only outward radiating elastic waves are allowed in the present problem. Hence, coefficient  $C$  in (4.7) is set equal to zero, yielding

$$U(r, f) = De^{-ikr} \left[ \frac{1}{kr} - \frac{i}{(kr)^2} \right]. \quad (5.1)$$

The remaining coefficient  $D$  is determined by imposing a boundary condition at the cavity wall. In the present section, an applied stress boundary condition is considered. In spherical polar coordinates, the stress tensor components for radial and spherically symmetric motion are

$$\sigma_{rr}(r, t) = (\lambda + 2\mu) \frac{\partial u(r, t)}{\partial r} + 2\lambda \frac{u(r, t)}{r}, \quad (5.2)$$

$$\sigma_{\theta\theta}(r, t) = \sigma_{\phi\phi}(r, t) = \lambda \frac{\partial u(r, t)}{\partial r} + 2(\lambda + \mu) \frac{u(r, t)}{r}, \quad (5.3)$$

$$\sigma_{\theta\phi}(r, t) = \sigma_{\phi r}(r, t) = \sigma_{r\theta}(r, t) = 0. \quad (5.4)$$

The boundary condition at the spherical interface  $r = a$  involves only the  $\sigma_{rr}$  tensor component. It is

$$\sigma_{rr}(a,t) = -s(t), \quad (5.5)$$

where  $s(t)$  is a prescribed function of time. In terms of the radial particle displacement, this boundary condition becomes

$$(\lambda + 2\mu) \left. \frac{\partial u(r,t)}{\partial r} \right|_{r=a} + 2\lambda \frac{u(a,t)}{a} = -s(t). \quad (5.6)$$

Fourier transforming equation (5.6) to remove the time dependence gives

$$(\lambda + 2\mu) \left. \frac{\partial U(r,f)}{\partial r} \right|_{r=a} + 2\lambda \frac{U(a,f)}{a} = -S(f), \quad (5.7)$$

where  $S(f)$  is the Fourier transform of the applied radial stress function  $s(t)$ . An expression for the derivative of the transformed displacement function  $U(r,f)$  is obtained from (5.1) above:

$$\frac{\partial U(r,f)}{\partial r} = kD e^{-ikr} \left[ \frac{2i}{(kr)^3} - \frac{2}{(kr)^2} - \frac{i}{kr} \right]. \quad (5.8)$$

Equations (5.1) and (5.8) are substituted into (5.7) and the resulting expressions is solved for the coefficient  $D$ . The analysis is simplified if the Lamé parameters  $\lambda$  and  $\mu$  are written in terms of the compressional and shear wavespeeds  $\alpha$  and  $\beta$  of the elastic medium:  $\lambda = \rho(\alpha^2 - 2\beta^2)$  and  $\mu = \rho\beta^2$ . The result is

$$D = \frac{a}{4\rho\beta^2} \left[ \frac{-i}{(ka)^2} + \frac{1}{ka} + \frac{i\alpha^2}{4\beta^2} \right]^{-1} e^{+ika} S(f). \quad (5.9)$$

## 6.0 FREQUENCY-DOMAIN SOLUTION

Substituting (5.9) into (5.1) and engaging in a certain amount of algebraic manipulation yields

$$U(r,f) = G(r,f)S(f), \quad (6.1)$$

where the *response function*  $G(r,f)$  is given by

$$G(r,f) = \frac{1}{i2\pi\rho\alpha} \left( \frac{a}{r} \right) \left[ \frac{f - Z_1(r)}{(f - P_1)(f - P_2)} \right] e^{-i2\pi f\tau(r)}. \quad (6.2)$$

Symbols in this expression are defined as follows:

$$\tau(r) = \frac{r-a}{\alpha}, \quad Z_1(r) = \frac{i\alpha}{2\pi r}, \quad (6.3a,b)$$

$$P_1 = \frac{\beta}{\pi a} \left[ \sqrt{1-\gamma^2} + i\gamma \right], \quad P_2 = \frac{\beta}{\pi a} \left[ -\sqrt{1-\gamma^2} + i\gamma \right], \quad (6.3c,d)$$

where  $\gamma \equiv \beta / \alpha$  is the ratio of S-wave to P-wave speed of the elastic medium.  $\gamma$  ranges from 0 to a maximum of  $\sqrt{3} / 2 \approx 0.866$  (assuming an elastic medium with negative Poisson ratio is allowed).  $\tau(r)$  is the travelttime of the elastic wave propagating from the cavity wall to radius  $r$  at the compressional wave speed  $\alpha$ .

The response function  $G(r,f)$  is analytically continued onto the complex plane by defining a complex-valued frequency  $F = f + ig$ , where  $f$  and  $g$  are real. Then, equation (6.2) indicates that  $P_1$  and  $P_2$  are poles and  $Z_1(r)$  is a zero of the continued response function  $G(r,F)$ . Since the poles are located in the upper half of the complex frequency plane, the associated time-domain impulse response is causal. Moreover, this time-domain response is minimum-delay [with respect to the arrival time  $\tau(r)$ ] because the zero  $Z_1(r)$  is also located in the upper half of the  $F$ -plane.

Interestingly, the response function  $G(r,f)$  has no zeros anywhere on the real frequency axis, except in the limit as  $r \rightarrow +\infty$ . Hence, all spectral components present in the source stress function  $s(t)$  (including the dc component) are radiated into the elastic wholespace. Finally, the response function (6.2) is consistent with an analogous frequency-domain expression given by Gurvich (1965).

## 7.0 TIME-DOMAIN SOLUTION

A time-domain expression for the radial particle displacement  $u(r,t)$  is obtained by inverse Fourier transforming equation (6.1).. Thus

$$u(r,t) = g(r,t) * s(t), \quad (7.1)$$

where the asterisk denotes convolution with respect to time  $t$ . The impulse response  $g(r,t)$  is the inverse Fourier transform of the response function  $G(r,f)$ :

$$g(r,t) = \int_{-\infty}^{+\infty} G(r,f) e^{+i2\pi f t} df. \quad (7.2)$$

This integral is evaluated via contour integration on the complex frequency plane. For time  $t$  greater than the arrival time  $\tau(r)$ , the contour is closed in the upper half plane; the residue theorem yields the contribution from the two poles  $P_1$  and  $P_2$ . The analysis is simplified by writing these poles as

$$P_1 = \frac{\omega_d}{2\pi} + i \frac{\alpha_d}{2\pi}, \quad P_2 = -\frac{\omega_d}{2\pi} + i \frac{\alpha_d}{2\pi}, \quad (7.3a,b)$$

where

$$\alpha_d \equiv \frac{2\beta}{a} \gamma, \quad \omega_d \equiv \frac{2\beta}{a} \sqrt{1-\gamma^2}. \quad (7.4a,b)$$

The motivation for adopting this particular choice of symbols will rapidly become apparent. The residues are given by

$$2\pi i \operatorname{res}[G(r, F)e^{+i2\pi Ft}; P_k] \equiv 2\pi i \lim_{F \rightarrow P_k} (F - P_k) G(r, F) e^{+i2\pi Ft} = \frac{(-1)^k a}{\rho \alpha r} \left[ \frac{P_k - Z_1(r)}{P_1 - P_2} \right] e^{+i2\pi P_k [t - \tau(r)]},$$

for  $k = 1, 2$ . Substituting in the expressions for the various quantities yields

$$2\pi i \operatorname{res}[G(r, F)e^{+i2\pi Ft}; P_1] = \frac{a}{2\rho\alpha r} e^{-\alpha_d [t - \tau(r)]} \left[ 1 + i \left( \frac{\alpha_d - \alpha/r}{\omega_d} \right) \right] e^{+i\omega_d [t - \tau(r)]},$$

$$2\pi i \operatorname{res}[G(r, F)e^{+i2\pi Ft}; P_2] = \frac{a}{2\rho\alpha r} e^{-\alpha_d [t - \tau(r)]} \left[ 1 - i \left( \frac{\alpha_d - \alpha/r}{\omega_d} \right) \right] e^{-i\omega_d [t - \tau(r)]}.$$

Thus, for  $t > \tau(r)$ , the integral in equation (7.2) evaluates to

$$g(r, t) = \frac{1}{\rho\alpha\sqrt{1-\gamma^2}} \left( \frac{a}{r} \right) e^{-\alpha_d [t - \tau(r)]} \left\{ \cos(\omega_d [t - \tau(r)] + \phi) + \frac{a}{2\gamma r} \sin(\omega_d [t - \tau(r)]) \right\}, \quad (7.5)$$

with  $\tan \phi \equiv \alpha_d / \omega_d = \gamma / \sqrt{1 - \gamma^2}$ . For  $t < \tau(r)$ , the integration contour is closed in the lower half of the complex  $F$ -plane, yielding  $g(r, t) = 0$ . Thus, the displacement impulse response is causal with respect to the time  $t = \tau(r)$ .

Expression (7.5) indicates that the displacement impulse response is an exponentially decaying oscillatory function;  $\alpha_d$  is a (angular) decay rate and  $\omega_d$  is a damped oscillation (angular) frequency. Note that the two terms of the oscillatory part of the response have different amplitudes and phases. Also,  $g(r, t)$  has the proper physical dimension for particle displacement response to an impulsive stress: reciprocal acoustic impedance. Finally, equation (7.5) is consistent with equivalent formulae in Eringen (1957) and Eringen and Suhubi (1975, p. 481).

Elastic particle velocity and acceleration are obtained from the displacement impulse response via

$$v(r, t) = \frac{\partial u(r, t)}{\partial t} = \frac{\partial g(r, t)}{\partial t} * s(t) = g(r, t) * \frac{\partial s(t)}{\partial t}, \quad (7.6)$$

$$a(r, t) = \frac{\partial v(r, t)}{\partial t} = \frac{\partial g^2(r, t)}{\partial t^2} * s(t) = g(r, t) * \frac{\partial^2 s(t)}{\partial t^2}. \quad (7.7)$$

The strain tensor components can be calculated via

$$\varepsilon_{rr}(r, t) = \frac{\partial u(r, t)}{\partial r} = \frac{\partial g(r, t)}{\partial r} * s(t), \quad (7.8)$$

$$\varepsilon_{\theta\theta}(r,t) = \varepsilon_{\phi\phi}(r,t) = \frac{u(r,t)}{r} = \frac{g(r,t)}{r} * s(t), \quad (7.9)$$

$$\varepsilon_{\phi\phi}(r,t) = \varepsilon_{\theta\theta}(r,t) = \varepsilon_{r\theta}(r,t) = 0. \quad (7.10)$$

Expressions for the stress tensor components in terms of the particle displacement are given in the previous section 5.0. The pressure at radius  $r$  is determined from the stress tensor components via

$$p(r,t) = -\frac{1}{3} [\sigma_{rr}(r,t) + \sigma_{\theta\theta}(r,t) + \sigma_{\phi\phi}(r,t)]. \quad (7.11)$$

Alternately, pressure is given by

$$p(r,t) = -k \operatorname{div} u(r,t) = -k \frac{1}{r^2} \frac{\partial}{\partial r} [r^2 u(r,t)] = -k \frac{1}{r^2} \frac{\partial}{\partial r} [r^2 g(r,t)] * s(t), \quad (7.12)$$

where  $k = \rho\alpha^2 [1 - (4/3)\gamma^2]$  is the bulk modulus of the elastic medium.

## 8.0 EXAMPLES AND APPLICATIONS

The examples discussed in this section assume that a spherical cavity is filled with an ideal fluid (i.e., a gas) with a time-varying pressure. Hence, the symbol  $p(t)$  is used instead of  $s(t)$  for the source activation function. Of course, for an ideal fluid, all three diagonal components of the stress tensor are equal ( $\sigma_{rr} = \sigma_{\theta\theta} = \sigma_{\phi\phi}$ ). Then, equation (7.11) indicates that this source pressure function is identical to the applied radial stress:  $p(t) = s(t)$ . A distinction between  $p(t)$  and  $s(t)$  is necessary in the situation where the spherical surface is located at the equivalent linear elastic radius  $r = a$  *within* a solid continuum.

### 8.1 Static Loading

Suppose that the cavity is subject to the static pressure  $p(t) = p_0$ . Then, the Fourier spectrum of this pressure function is impulsive:  $P(f) = p_0 \delta(f)$ , where  $\delta(f)$  is a Dirac delta function. Substituting  $P(f)$  for  $S(f)$  in equation (6.1) and (trivially) performing the inverse Fourier transform results in

$$u(r,t) = u_0(r) = \frac{p_0 a}{4\rho\beta^2} \left(\frac{a}{r}\right)^2 = \frac{p_0 a}{4\mu} \left(\frac{a}{r}\right)^2. \quad (8.1)$$

Interestingly, the static particle displacement  $u_0(r)$  does not depend on the P-wave speed  $\alpha$  or the Lamé coefficient  $\lambda$  of the elastic medium.

The total source pressure function often consists of static and dynamic parts:  $p_{\text{total}}(t) = p_0 + p(t)$ . Linear superposition then implies that  $u(r,t) = g(r,t) * p(t)$  is a time-varying radial displacement *relative* to the static component  $u_0(r)$ .

## 8.2 Explosive Loading

An applied pressure of the form  $p(t) = p_0 H(t) \exp(-\kappa t)$  (where  $H(t)$  is the Heaviside unit step function) approximates explosive loading of the cavity wall (Sharpe, 1942; Blake, 1952, Goldsmith and Allen, 1955; Peet, 1960). An expression for the radial displacement can be obtained by convolving this pressure function with the impulse response  $g(r,t)$  in equation (7.5). Persisting through a major amount of algebraic reduction yields

$$u(r,t) = \frac{1}{\rho\alpha\sqrt{1-\gamma^2}} \frac{p_0}{\sqrt{(\alpha_d - \kappa)^2 + \omega_d^2}} \left(\frac{a}{r}\right) \times$$

$$\left\{ e^{-\alpha_d[t-\tau(r)]} \left[ \sin(\omega_d[t-\tau(r)] + \phi - \theta) - \frac{a}{2\gamma r} \cos(\omega_d[t-\tau(r)] - \theta) \right] \right.$$

$$\left. - e^{-\kappa[t-\tau(r)]} \left[ \sin(\phi - \theta) - \frac{a}{2\gamma r} \cos(\theta) \right] \right\} H[t - \tau(r)], \quad (8.2)$$

where  $\tan \theta \equiv (\alpha_d - \kappa)/\omega_d$ . At a fixed radius  $r$ , the particle displacement consists of an exponential term which decays at the same rate as the forcing function, plus a damped oscillatory transient. Although the applied pressure function is discontinuous at  $t = 0$ , expression (8.2) indicates that the particle displacement is continuous at the onset of the arriving compressional wave:  $u[r, \tau(r)] = 0$ , as expected. However, the particle velocity has a step discontinuity and the particle acceleration is impulsive at onset time  $t = \tau(r)$ . Sharpe (1942) and Duvall (1953) demonstrate that the velocity discontinuity is removed by considering a pressure of the form  $p(t) = p_0 H(t) [\exp(-\kappa_1 t) - \exp(-\kappa_2 t)]$ . The results for this particular pressure can be obtained from equation (8.2) via superposition.

In the limit as  $\kappa \rightarrow 0$ , expression (8.2) gives the response to a finite step in cavity pressure:

$$u(r,t) = \frac{p_0 a}{4\rho\beta^2} \left(\frac{a}{r}\right) \times$$

$$\left\{ \left(\frac{a}{r}\right) + \frac{2\gamma}{\sqrt{1-\gamma^2}} e^{-\alpha_d[t-\tau(r)]} \left[ \sin(\omega_d[t-\tau(r)]) - \frac{a}{2\gamma r} \cos(\omega_d[t-\tau(r)] - \phi) \right] \right\} H[t - \tau(r)]. \quad (8.3)$$

As a check, note that the static displacement (8.1) is recovered as  $t \rightarrow +\infty$ . Equation (8.3) is consistent with results in Jeffreys (1931), Sharpe (1942), Blake (1952), Miklowitz (1978, p. 281), Ben-Menahem and Singh (1981, p. 223), and Denny and Johnson (1991). In contrast, analogous formulae in Kawasumi and Yosiyama (1935) and Graff (1975, p. 298) contain a discontinuity at  $t = \tau(r)$  and hence are erroneous. The expression in Eringen and Suhubi (1975, p. 482) appears to be seriously in error: in addition to being dimensionally incorrect, it does not approach the static displacement  $u_0(r)$  at large times.

### 8.3 Acoustic Medium

Although the wholespace is assumed to be a linearly elastic solid, the correct results for an ideal fluid medium can be obtained by taking the limit of the relevant expressions as the shear wave velocity  $\beta$  approaches zero. The particle displacement impulse response in equation (7.5) becomes

$$b(r, t) \equiv \lim_{\beta \rightarrow 0} g(r, t) = \frac{1}{\rho\alpha} \left( \frac{a}{r} \right) \left\{ 1 + \frac{\alpha[t - \tau(r)]}{r} \right\} H[t - \tau(r)]. \quad (8.4)$$

Convolving  $b(r, t)$  with the applied pressure yields the radial displacement  $u(r, t)$  in an ideal fluid medium. However, the particle velocity is often of greater interest in acoustic problems. Differentiating the above expression and convolving the result with the pressure  $p(t)$  yields

$$v(r, t) = \frac{1}{\rho\alpha} \left( \frac{a}{r} \right) \left\{ p[t - \tau(r)] + \frac{\alpha}{r} \int_{-\infty}^{t - \tau(r)} p(x) dx \right\}. \quad (8.5)$$

The first term of the particle velocity is directly proportional to the source pressure function, after accounting for propagation delay. The second term is often called the afterflow term (Kramer, et al., 1968), and is relatively important at small ranges  $r$ .

### 8.4 Far-Field Approximation

At large distances from the cavity center, the expression for the particle displacement impulse response can be simplified. Consider the response function  $G(r, f)$  in equation (6.2). If  $|f| \gg |Z_1(r)| = \alpha / 2\pi r$ , then

$$G(r, f) \approx G_{far}(r, f) = \frac{1}{i2\pi\rho\alpha} \left( \frac{a}{r} \right) \left[ \frac{f}{(f - P_1)(f - P_2)} \right] e^{-i2\pi f \tau(r)}. \quad (8.6)$$

This *far-field* representation is valid when  $r \gg \alpha / 2\pi|f| = \lambda_\alpha / 2\pi$ , where  $\lambda_\alpha \equiv \alpha / |f|$  is the wavelength of compressional elastic radiation with frequency  $f$ . Thus, the distance to the far-field realm is wavelength (or frequency) dependent. The inverse Fourier transform of the above response function is

$$g_{far}(r, t) = \frac{1}{\rho\alpha\sqrt{1 - \gamma^2}} \left( \frac{a}{r} \right) e^{-\alpha_d[t - \tau(r)]} \cos(\omega_d[t - \tau(r)] + \phi) H[t - \tau(r)]. \quad (8.7)$$

Hence, the far-field impulse response is a damped sinusoidal oscillation that propagates without change in form, except for spherical divergence. In fact, the waveform in (8.7) is a Berlage wavelet of order zero (Aldridge, 1990).

Note that the far-field response function  $G_{far}(r, f)$  has a zero at  $f = 0$ . Thus, the dc component of the cavity pressure  $p(t)$  is not radiated into the far-field.

### 8.5 Point source

Let a dimensionless source waveform be defined as  $q(t) \equiv p(t)/p_0$ , where  $p_0$  is a positive measure of the cavity pressure  $p(t)$ . For example,  $p_0$  could be the root-mean-square value of  $p(t)$ , or the maximum absolute value of  $p(t)$ , etc. A *point source* of compressional elastic radiation is obtained in the limit as the

radius of the cavity  $a$  tends to zero and the pressure  $p(t)$  tends to infinity, in such a manner that the quantity  $E_0 \equiv 4\pi a^3 p_0 / 3$  remains finite. Note that  $E_0$  has physical dimension of energy. Under these conditions, it is straightforward to demonstrate that the Fourier transformed particle displacement in equation (6.1) approaches

$$U_p(r, f) = \frac{3E_0}{16\pi\mu} \left[ \frac{i2\pi f}{\alpha r} + \frac{1}{r^2} \right] e^{-i2\pi f r / \alpha} Q(f). \quad (8.8)$$

Inverse Fourier transforming this expression yields

$$u_p(r, t) = \frac{3E_0}{16\pi\mu} \left[ \frac{q'(t - r/\alpha)}{\alpha r} + \frac{q(t - r/\alpha)}{r^2} \right]. \quad (8.9)$$

Hence, the particle displacement waveform generated by a point compressional source changes shape from the near-field to the far-field. In the far-field, it has the shape of the derivative of the source pressure pulse. Equation (8.9) agrees with the expression obtained by Ben-Menahem and Singh (1981, p. 223).

## 8.6 Scaling Relations

The frequency response  $G(r, f)$  and the impulse response  $g(r, t)$  depend on the cavity radius  $a$ . How do these quantities change if the radius is scaled by a multiplicative constant? Let the dependence of the responses on  $a$  be denoted explicitly by  $G(r, f; a)$  and  $g(r, t; a)$ . Then, from equation (6.2), it is straightforward to demonstrate that

$$G(r, f; ca) = cG(r/c, cf; a), \quad (8.10)$$

where  $c$  is a real and positive scalar. Inverse Fourier transforming this expression yields

$$g(r, t; ca) = g(r/c, t/c; a). \quad (8.11)$$

Interestingly, this scaling relation also applies to the far-field impulse response of equation (8.7):

$$g_{far}(r, t; ca) = g_{far}(r/c, t/c; a). \quad (8.12)$$

These scaling relations underlie many “charge size scaling laws” used for analysis of explosion seismic data (e.g., Latter, et al., 1959; Peet, 1960; Ziolkowski, et al., 1980; Denny and Johnson, 1991; Ziolkowski, 1993; Ziolkowski and Bokhorst, 1993). In this context,  $a$  is *not* considered to be the radius of the charge or of the underground cavity excavated by the explosion. Rather,  $a$  is taken to be the radius of a larger spherical cavity on which deformations, stresses, and strains have decayed to a level where linear elasticity applies (Sharpe, 1942).

## 9.0 RADIATED ENERGY

The total energy radiated away from the spherical cavity can be calculated from the energy balance principle of continuum mechanics. In the purely mechanical theory, there are no thermodynamic terms involved. Thus, the energy balance principle reduces to

Rate of change of energy = Rate of work done by body and contact forces.

In the current problem, body forces are neglected. The rate of work done by contact forces is given by the integral of  $\mathbf{T} \cdot \mathbf{v}$  over the boundary  $\partial A$  of the elastic medium, where  $\mathbf{T}$  and  $\mathbf{v}$  are surface traction and particle velocity vectors, respectively. Hence, the energy balance principle can be expressed mathematically as

$$\frac{d\mathcal{E}(t)}{dt} = \int_{\partial A} \mathbf{T} \cdot \mathbf{v} dA, \quad (9.1)$$

where  $\mathcal{E}(t)$  is the energy of the elastic body. This energy consists of kinetic energy  $\mathcal{K}(t)$  and potential energy (strain energy)  $\mathcal{W}(t)$ . For the present spherically symmetric problem, the surface integral in (9.1) is readily evaluated, giving

$$\frac{d\mathcal{E}(t)}{dt} = 4\pi a^2 s(t) v(a, t). \quad (9.2)$$

Integrating this expression with respect to time yields

$$\mathcal{E}(t) = 4\pi a^2 \int_{-\infty}^t s(x) v(a, x) dx. \quad (9.3)$$

Finally, the total energy radiated into the elastic wholespace is given by  $E \equiv \lim_{t \rightarrow \infty} \mathcal{E}(t)$ . Thus

$$E = 4\pi a^2 \int_{-\infty}^{+\infty} s(t) v(a, t) dt. \quad (9.4)$$

The energy expression (9.4) can be simplified. The Fourier transform of the cavity wall velocity  $v(a, t)$  is  $V(a, f) = (i2\pi f) U(a, f) = (i2\pi f) G(a, f) S(f)$ . Then, applying the power theorem (Bracewell, 1965, p.113) to equation (9.4) gives

$$E = 4\pi a^2 \int_{-\infty}^{+\infty} |S(f)|^2 (i2\pi f)^* G(a, f)^* df, \quad (9.5)$$

where the asterisk denotes complex conjugation. The total radiated energy depends on the energy density spectrum  $|S(f)|^2$  of the source stress waveform. The inverse Fourier transform of the energy density spectrum is the autocorrelation function  $\phi_{ss}(t) = s(t) * s(-t)$ . Hence, utilizing the power theorem once again yields

$$E = 4\pi a^2 \int_{-\infty}^{+\infty} \phi_{ss}(t) \frac{\partial g(a, t)}{\partial t} dt. \quad (9.6)$$

This is an appealing result; the total radiated energy depends on the autocorrelation function of the source waveform, rather than on the waveform itself. A normalized autocorrelation is defined as  $\hat{\phi}_{ss}(t) \equiv \phi_{ss}(t)/\phi_{ss}(0)$ . Then, substituting expression (7.5) for the displacement impulse response into the above equation gives

$$E = \frac{4\pi a^2 \phi_{ss}(0)}{\rho \alpha} \left\{ 1 + \frac{2\beta}{a} \int_0^{+\infty} \hat{\phi}_{ss}(t) e^{-\alpha t} [D_1 \cos \omega_d t + D_2 \sin \omega_d t] dt \right\}, \quad (9.7)$$

where  $D_1$  and  $D_2$  are constants that depend on the wavespeed ratio  $\gamma$ :

$$D_1 = \frac{1}{2\gamma} - 2\gamma, \quad D_2 = \frac{2(\gamma^2 - 3/4)}{\sqrt{1 - \gamma^2}}. \quad (9.8a,b)$$

For geological media where  $\gamma \approx 1/2$ , then  $D_1 = 0$  and  $D_2 = -2/\sqrt{3}$ . Curiously, if  $\gamma = \sqrt{3}/2 \approx 0.866$  (the theoretical maximum value corresponding to a Poisson ratio of  $-1$ ), then the roles of  $D_1$  and  $D_2$  are reversed:  $D_1 = -2/\sqrt{3}$  and  $D_2 = 0$ .

## 9.1 Explosive Loading

The general energy expression (9.7) simplifies dramatically in the particular case where the source radial stress waveform is given by  $s(t) = s_0 H(t) \exp(-\kappa t)$ . As indicated previously, this stress approximates explosive loading of the cavity wall. The autocorrelation function is  $\phi_{ss}(t) = (s_0^2/2\kappa) \exp(-\kappa|t|)$ . Then, equation (9.7) reduces to

$$E = \frac{3V_0 s_0^2}{8\mu} \frac{1}{1 + \kappa^2 / (\omega_c^2 + 2\gamma\omega_c \kappa)}, \quad (9.9)$$

where  $V_0 = 4\pi a^3 / 3$  is the volume of the spherical cavity and  $\omega_c$  is a characteristic angular frequency defined by  $\omega_c \equiv \sqrt{(\alpha_d^2 + \omega_d^2)} = 2\beta/a$ . In the limit as  $\kappa \rightarrow 0$ ,  $E$  approaches the value  $3V_0 s_0^2 / 8\mu$ , which is the strain energy associated with the static displacement field  $u_0(r)$ . Interestingly, this same value is obtained by Denny and Johnson (1991) by considering *only* the far-field displacement. Also, note the  $E$  in (9.9) vanishes as the cavity radius  $a$  approaches zero, as expected.

Now consider an applied stress of the form  $s(t) = s_0 H(t) [\exp(-\kappa_1 t) - \exp(-\kappa_2 t)]$ . This function is continuous, and is thus a more realistic representation of a physical stress waveform. The autocorrelation function of  $s(t)$  is

$$\phi_{ss}(t) = \frac{s_0^2}{2} \left[ \frac{\kappa_2 - \kappa_1}{\kappa_2 + \kappa_1} \right] \left[ \frac{e^{-\kappa_1|t|}}{\kappa_1} - \frac{e^{-\kappa_2|t|}}{\kappa_2} \right]. \quad (9.10)$$

Except for a multiplicative scaling factor, expression (9.10) equals the difference between two autocorrelation functions of the form used in the derivation of the previous energy expression (9.9). Hence, the total energy radiated into the wholespace can be written down by inspection of (9.9). The result is

$$E = \frac{3V_0 s_0^2}{8\mu} \left[ \frac{\kappa_2 - \kappa_1}{\kappa_2 + \kappa_1} \right] \left[ \frac{Q_1(\kappa_1)}{Q_2(\kappa_1)} - \frac{Q_1(\kappa_2)}{Q_2(\kappa_2)} \right], \quad (9.11)$$

where  $Q_1(\kappa)$  and  $Q_2(\kappa)$  are polynomials given by

$$Q_1(\kappa) = \omega_c^2 + 2\gamma\omega_c \kappa, \quad Q_2(\kappa) = \omega_c^2 + 2\gamma\omega_c \kappa + \kappa^2. \quad (9.12a,b)$$

In the limit as  $\kappa_1 \rightarrow 0$ , the stress becomes  $s(t) = s_0 H(t) [1 - \exp(-\kappa_2 t)]$ . This stress exponentially approaches the static value  $s_0$  at large times. Sezawa (1935) and Sezawa and Kanai (1936) use this form of  $s(t)$  to study the dependence of the radiated energy on the ‘‘rapidity’’ of the radial stress application at the cavity wall. Setting  $\kappa_1 = 0$  in (9.11) yields

$$E = \frac{3V_0 s_0^2}{8\mu} \frac{\kappa_2^2}{\omega_c^2 + 2\gamma\omega_c \kappa_2 + \kappa_2^2}. \quad (9.13)$$

This expression is consistent with results in Sezawa and Kanai (1936). Note that  $E$  vanishes as  $\kappa_2 \rightarrow 0$ , and  $E$  approaches the static deformation value as  $\kappa_2 \rightarrow +\infty$ , as expected.

## 9.2 Energy Scaling

The above formulae clearly indicate that the total elastic energy radiated from a spherical cavity source depends on the radius of the cavity. However, the problem of how the energy changes if the cavity radius is scaled by a multiplicative factor is somewhat subtle. In order to examine this issue, rewrite one of the above general energy expressions so that all relevant quantities depend explicitly on the cavity radius  $a$ . Thus, the frequency-domain expression (9.5) is re-written in the form

$$E(a) = 4\pi a^2 \int_{-\infty}^{+\infty} |S(f; a)|^2 (i2\pi f)^* G(a, f; a)^* df. \quad (9.14)$$

Recall that  $G(r, f; a)$  is the response function (Fourier transform of the displacement impulse response) at distance  $r$  and frequency  $f$ , for a cavity source of radius  $a$ . Thus  $G(a, f; a)$  is the response function evaluated at the particular radius  $r = a$  (i.e., at the cavity wall). For a cavity with radius  $ca$  (where  $c$  is a positive scalar), the radiated energy is

$$E(ca) = 4\pi (ca)^2 \int_{-\infty}^{+\infty} |S(f; ca)|^2 (i2\pi f)^* G(ca, f; ca)^* df. \quad (9.15)$$

Utilizing the scaling relation (8.10), the above expression is put into the form

$$E(ca) = c 4\pi a^2 \int_{-\infty}^{+\infty} |S(f/c; ca)|^2 (i2\pi f)^* G(a, f; a)^* df. \quad (9.16)$$

Thus, in order to determine an energy scaling relation, an additional assumption must be adopted regarding the scaling properties of the source stress spectrum  $S(f; a)$ . If this spectrum obeys the scaling rule

$$S(f/c; ca) = c^n S(f; a), \quad (9.17)$$

where  $n$  is an (not necessarily integer) exponent, then equation (9.16) reduces to

$$E(ca) = c^{2n+1} E(a). \quad (9.18)$$

The total radiated elastic energy exhibits a power-law dependence on the cavity radius  $a$ .

An alternative way of writing the source spectrum scaling rule (9.17) is

$$S(f; ca) = c^n S(cf; a). \quad (9.19)$$

Inverse Fourier transforming this relation to the time-domain yields

$$s(t; ca) = c^{n-1} s(t/c; a). \quad (9.20)$$

Source radial stress functions of the form  $s(t) = s_0 H(t) \exp(-\kappa_1 t)$ , or  $s(t) = s_0 H(t) [\exp(-\kappa_1 t) - \exp(-\kappa_2 t)]$ , or  $s(t) = s_0 H(t) [1 - \exp(-\kappa_2 t)]$  obey the scaling rule (9.20) provided (i) the magnitude scalar  $s_0$  is proportional to  $a^{n-1}$ , and (ii) the exponential decay rates  $\kappa_1, \kappa_2$  are inversely proportional to  $a$ . Clearly, the particular choice  $n = 1$  leads to the simplified results

$$E(ca) = c^3 E(a), \quad s(t; ca) = s(t/c; a), \quad s_0 \text{ independent of } a.$$

In this case, the total radiated elastic energy scales as the cube of the cavity radius. The shock wave theory described by Peet (1960) for the development of a spherical nonlinearly deformed zone around a buried explosion takes  $n = 1$ .

## 10.0 INVERSE IMPULSE RESPONSE

The particle displacement impulse response  $g(r, t)$  is minimum delay with respect to the arrival time  $\tau(r)$ . Hence, it is possible to derive a stable inverse  $g^{-1}(r, t)$  that can be used to deconvolve a recorded particle displacement seismogram. From equation (7.1), the convolution of  $g^{-1}(r, t)$  with  $u(r, t)$  yields the radial stress waveform  $s(t)$  applied to the cavity wall:

$$g^{-1}(r, t) * u(r, t) = g^{-1}(r, t) * g(r, t) * s(t) = \delta(t) * s(t) = s(t).$$

The Fourier transform of the inverse impulse response is the reciprocal of the response function  $G(r, f)$  in equation (6.2):

$$G^{-1}(r, f) = G(r, f)^{-1} = i2\pi\rho\alpha \left( \frac{r}{a} \right) \left[ \frac{(f - P_1)(f - P_2)}{f - Z_1(r)} \right] e^{+i2\pi f\tau(r)}. \quad (10.1)$$

Hence,  $G^{-1}(r, f)$  has a single pole in the upper half of the complex frequency plane at  $F = Z_1(r)$ . The inverse Fourier transform of (10.1) can be calculated using the residue theorem. However, care must be

exercised because  $G^{-1}(r,f)$  is not uniformly convergent as  $|F| \rightarrow +\infty$ . This difficulty is overcome by applying the residue theorem to the quantity

$$\left[ G^{-1}(r,F) - \rho\alpha \left( \frac{r}{a} \right) (i2\pi F) e^{+i2\pi F \tau(r)} \right] e^{+i2\pi Ft},$$

which approaches zero uniformly as  $|F| \rightarrow +\infty$ . The result is

$$g^{-1}(r,t) = \rho\alpha \left( \frac{r}{a} \right) \left\{ \delta'[t + \tau(r)] + \left[ \omega_d^2 + (\alpha_d - \alpha/r)^2 \right] e^{-\alpha[t + \tau(r)]/r} H[t + \tau(r)] \right\}, \quad (10.2)$$

where  $\delta'(t)$  is the derivative of the Dirac delta function. The inverse impulse response is causal with respect to the time  $t = -\tau(r)$ . It is possible to verify that  $g^{-1}(r,t) * g(r,t) = \delta(t)$ , as is required. Also, analysis indicates that  $g^{-1}(r,t)$  diverges as  $r \rightarrow +\infty$ . This is consistent with the fact that the Fourier amplitude spectrum of the far-field impulse response has a zero at  $f = 0$  Hz.

Convolving  $g^{-1}(r,t)$  in (10.2) with the radial displacement  $u(r,t)$  gives

$$s(t) = \rho\alpha \left( \frac{r}{a} \right) \left\{ v[r, t + \tau(r)] + \left[ \omega_d^2 + (\alpha_d - \alpha/r)^2 \right] e^{-\alpha[t + \tau(r)]/r} \int_{-\infty}^{t + \tau(r)} u(r, x) e^{+\alpha x/r} dx \right\}, \quad (10.3)$$

where  $v(r,t)$  is the elastic particle velocity.

## 11.0 ART REPRESENTATION

The response function  $G(r,F)$  of equation (6.2) is analytic everywhere on the complex frequency plane except at the two poles  $P_1$  and  $P_2$ . Thus, it is possible to derive various power series representations for this response function. An expansion of  $G(r,F)$  in negative powers of complex frequency  $F$  is convergent in the infinite annulus  $|F| > |P_1| = |P_2| = \beta/\pi a$ , and yields the *asymptotic ray theory* (ART) representation of the response function.

Since the problem under investigation has an exact solution (in the form of equation (6.2) in the frequency-domain or equation (7.5) in the time-domain), the ART representation would seem to be of limited utility. However, the following development does illustrate one important point: the ART solution is mathematically exact for all ranges  $r > a$  and all frequencies  $f$  exceeding the *finite* cutoff value  $f_c = \omega_c/2\pi = \beta/\pi a$ . The commonly held notion that the ART solution is valid only for "infinite frequency" is erroneous. The ART expansion obtained below for the spherical cavity problem is also useful for comparison with other ART solutions.

Consider the factor  $1/(f - P_1)$  in the response function  $G(r,f)$ . This factor can be expressed as an infinite series in negative powers of frequency  $f$  as follows:

$$\frac{1}{f - P_1} = \frac{1}{f(1 - P_1/f)} = \frac{1}{f} \sum_{k=0}^{\infty} \left( \frac{P_1}{f} \right)^k = \frac{1}{f} \sum_{k=0}^{\infty} P_1^k f^{-k}.$$

This series converges for  $|P_1/f| < 1$ , or equivalently for  $|f| > |P_1| = \beta/\pi a$ . Similarly

$$\frac{1}{f - P_2} = \frac{1}{f} \sum_{k=0}^{\infty} P_2^k f^{-k},$$

if  $|f| > |P_2| = \beta/\pi a$ . Multiplying these two infinite series together yields

$$\frac{1}{(f - P_1)(f - P_2)} = \frac{1}{f^2} \sum_{k=0}^{\infty} b_k f^{-k}, \quad (11.1)$$

where  $b_k \equiv \sum_{n=0}^k P_1^{k-n} P_2^n$ . These coefficients can be evaluated in closed form as follows:

$$b_k = P_1^k \sum_{n=0}^k (P_2/P_1)^n = P_1^k \left[ \frac{1 - (P_2/P_1)^{k+1}}{1 - (P_2/P_1)} \right] = \frac{P_1^{k+1} - P_2^{k+1}}{P_1 - P_2}.$$

Using  $P_1 = +(\beta/\pi a) \exp(+i\phi)$  and  $P_2 = -(\beta/\pi a) \exp(-i\phi)$  gives

$$b_k = \frac{1}{2\sqrt{1-\gamma^2}} \left( \frac{\beta}{\pi a} \right)^k \left[ e^{+i(k+1)\phi} + (-1)^k e^{-i(k+1)\phi} \right].$$

Substituting the series (11.1) into the expression for the response function  $G(r,f)$  and engaging in a certain amount of manipulation yield the ART representation of the (Fourier transformed) elastic particle displacement:

$$U(r, f) = \frac{aS(f)}{\rho\alpha^2\sqrt{1-\gamma^2}} \left[ \sum_{k=1}^{\infty} u_k(r) (i2\pi f)^{-k} \right] e^{-i2\pi f \tau(r)}, \quad (11.2)$$

where the *amplitude coefficients* of the expansion are given by

$$u_k(r) = c_{k-1} \left( \frac{\alpha}{r} \right) + c_{k-2} \left( \frac{\alpha}{r} \right)^2. \quad (11.3)$$

The coefficients  $c_k$  are defined as

$$c_k = (i2\pi f_c)^k \begin{cases} \cos[(k+1)\phi], & k \text{ even,} \\ i \sin[(k+1)\phi], & k \text{ odd,} \end{cases} \quad (11.4)$$

and  $c_{-1} = 0$ . Recall that  $f_c = \beta/\pi a$  and  $\tan \phi = \gamma/\sqrt{1-\gamma^2}$ . The amplitude coefficients are real-valued and have physical dimensions of (frequency)<sup>k</sup>, so that each term in the infinite sum is dimensionless. Also, note that there is no zeroth-order term in the sum. Finally, as, expected, the *phase function* of the ART expansion is  $\tau(r) = (r - a)/\alpha$ .

It is emphasized that the series (11.2) is convergent, and not merely asymptotic, for all frequencies exceeding  $f_c$  is absolute value.

The *first-order* ART approximation is obtained by retaining only the  $k = 1$  term in sum (11.2) above:

$$U(r, f) = \frac{1}{\rho\alpha} \left( \frac{a}{r} \right) \frac{S(f)}{(i2\pi f)} e^{-i2\pi f\tau(r)},$$

or alternately

$$V(r, f) = \frac{1}{\rho\alpha} \left( \frac{a}{r} \right) S(f) e^{-i2\pi f\tau(r)}, \quad (11.5)$$

where  $V(r, f)$  is the Fourier transformed radial particle velocity. Equation (11.5) indicates that the far-field radial velocity waveform is a scaled and delayed version of the source radial stress waveform.

In the limit as the shear wave speed  $\beta$  approaches zero, the amplitude coefficients  $u_k(r)$  vanish for  $k > 2$ , and the series (11.2) reduces to

$$U(r, f) = \frac{aP(f)}{\rho\alpha^2} \left[ \sum_{k=1}^2 u_k(r) (i2\pi f)^{-k} \right] e^{-i2\pi f\tau(r)}, \quad (11.6)$$

with  $u_1(r) = \alpha / r$  and  $u_2(r) = (\alpha / r)^2$ . [Note that the (Fourier transformed) source radial stress  $S(f)$  is replaced by a source pressure  $P(f)$  for an ideal fluid medium.] The ART expansion for spherically diverging acoustic waves in a homogeneous medium contains only two terms, in agreement with the previous expression (8.5). This result can also be derived directly from the response function  $G(r, f)$  of equation (6.2) when  $\beta \rightarrow 0$ . In this case, the poles  $P_1$  and  $P_2$  move to the origin of the complex frequency plane, and the series (11.2) is convergent for *all* nonzero frequencies.

## 12.0 DISPLACEMENT BOUNDARY CONDITION

The foregoing analysis is restricted to the case where a radial stress  $s(t)$  [or a pressure  $p(t)$ ] is applied to the cavity wall. An alternate boundary condition at  $r = a$  entails a prescribed radial displacement  $u(a, t)$ . The resulting outward propagating spherical waves are still described by equation (5.1); coefficient  $D$  is easily determined from the displacement boundary condition. The solution to this particular formulation of the problem is summarized in this section. In general, the expressions are simpler than the analogous expressions for the stress boundary condition.

### 12.1 Frequency-Domain Solution

Evaluating (5.1) at  $r = a$  and solving for the coefficient  $D$  yields

$$D = \left[ \frac{1}{ka} - \frac{i}{(ka)^2} \right]^{-1} e^{+ika} U(a, f), \quad (12.1)$$

where  $U(a,f)$  is the Fourier transform of the prescribed radial particle displacement  $u(a,t)$ . Substituting this result back into (5.1) gives

$$U(r, f) = H(r, f) U(a, f), \quad (12.2)$$

where the *response function*  $H(r,f)$  is defined as

$$H(r, f) = \left(\frac{a}{r}\right) \left[ \frac{f - Z_1(r)}{f - Z_1(a)} \right] e^{-i2\pi f \tau(r)}. \quad (12.3)$$

The analytically continued response function  $H(r,F)$  has a zero  $Z_1(r) = i\alpha/2\pi r$  and a pole  $Z_1(a) = i\alpha/2\pi a$  on the complex frequency plane. Since these are both located in the upper half of the  $F$ -plane, the associated time domain impulse response is causal and minimum delay [with respect to the arrival time  $\tau(r) = (r - a)/\alpha$ ].

## 12.2 Time-Domain Solution

A time-domain expression for the radial particle displacement is obtained by inverse Fourier transforming equation (12.2):

$$u(r, t) = h(r, t) * u(a, t). \quad (12.4)$$

The impulse response  $h(r,t)$  is the inverse Fourier transform of the frequency response  $H(r,f)$ . Applying the residue theorem to the quantity  $H(r,f) - (a/r) \exp[-i2\pi F \tau(r)]$  yields

$$h(r, t) = \left(\frac{a}{r}\right) \left\{ \delta[t - \tau(r)] - \frac{\alpha}{a} \left(1 - \frac{a}{r}\right) e^{-\alpha[t - \tau(r)]/a} H[t - \tau(r)] \right\}. \quad (12.5)$$

Finally, convolving (12.5) with the applied displacement function  $u(a,t)$  gives

$$u(r, t) = \left(\frac{a}{r}\right) \left\{ u[a, t - \tau(r)] - \frac{\alpha}{a} \left(1 - \frac{a}{r}\right) e^{-\alpha[t - \tau(r)]/a} \int_{-\infty}^{t - \tau(r)} u(a, x) e^{+\alpha x/a} dx \right\}. \quad (12.6)$$

The first term in the particle displacement solution represents the familiar amplitude decay due to spherical divergence. The second term indicates that the displacement waveform undergoes a progressive change in shape as it propagates outward.

## 12.3 Static, Step, and Exponential Displacements

Suppose that the static displacement  $u(a,t) = u_0$  is applied to the cavity wall. Then, the Fourier transformed displacement is impulsive:  $U(a,f) = u_0 \delta(f)$ . The inverse Fourier transform of  $U(r,f)$  is easily evaluated, giving

$$u(r, t) = u_0(r) = u_0 \left(\frac{a}{r}\right)^2. \quad (12.7)$$

This result is consistent with the previous equation (8.1) if  $u_0$  is taken to be  $p_0 a / 4\mu$ .

Now assume that the cavity wall is subject to the step displacement  $u(a,t) = u_0 H(t)$ . Evaluation of equation (12.6) with this boundary displacement yields

$$u(r,t) = u_0 \left( \frac{a}{r} \right) \left[ \left( \frac{a}{r} \right) + \left( 1 - \frac{a}{r} \right) e^{-\alpha[t-\tau(r)]/a} \right] H[t - \tau(r)]. \quad (12.8)$$

As  $t \rightarrow +\infty$ , this expression approaches the static displacement (12.7). Although this step response is a mathematically correct solution of the general displacement equation, one should not invest too much physical significance in the result. Propagating displacement discontinuities [ $u(r,t)$  in (12.8) is discontinuous at the arrival time  $t = \tau(r)$ ] are not admissible within the context of continuum mechanics. Rather (12.8) should be understood as a limiting situation.

Finally, consider the exponentially decaying applied displacement  $u(a,t) = u_0 \exp(-\kappa t) H(t)$ . Evaluating (12.6) yields

$$u(r,t) = u_0 \left( \frac{a}{r} \right) \left\{ \left[ \frac{\alpha/r - \kappa}{\alpha/a - \kappa} \right] e^{-\kappa[t-\tau(r)]} - \left[ \frac{\alpha/r - \alpha/a}{\alpha/a - \kappa} \right] e^{-\alpha[t-\tau(r)]/a} \right\} H[t - \tau(r)]. \quad (12.9)$$

The indeterminacy in this expression that arises when  $\kappa = \alpha/a$  is easily treated. Note that (12.9) also has a discontinuity at  $t = \tau(r)$ .

#### 12.4 Point Source

A dimensionless displacement waveform applied to the cavity wall can be defined as  $q(t) \equiv u(a,t) / u_0$ , where  $u_0$  is a positive measure of  $u(a,t)$ . Then, a point source compressional elastic waves is obtained in the limit as the cavity radius  $a$  vanishes and the source displacement  $u(a,t)$  grows without bound, in such a manner that the product  $V_s \equiv 4\pi a^2 u_0$  remains finite. Note that  $V_s$  has physical dimension volume. However,  $V_s$  is not the cavity volume; rather, it is additional volume “injected” by the radial displacement source into the elastic wholespace. Under these conditions, equations (12.2) and (12.3) approach

$$U_p(r, f) = \frac{V_s}{4\pi} \left[ \frac{i2\pi f}{\alpha r} + \frac{1}{r^2} \right] e^{-i2\pi f r / \alpha} Q(f). \quad (12.10)$$

Inverse Fourier transforming this expression yields the time-domain displacement

$$u_p(r, t) = \frac{V_s}{4\pi} \left[ \frac{q'(t - r/\alpha)}{\alpha r} + \frac{q(t - r/\alpha)}{r^2} \right]. \quad (12.11)$$

The mathematical structure of the above two expressions is identical to that of the previous equations (8.8) and (8.9) obtained for a point source with stress boundary conditions! Thus, in the limiting case of a point compressional source, the details of the applied boundary conditions (stress or displacement) become irrelevant.

## 12.5 Scaling Relations

The frequency-domain and time-domain response functions obey scaling relations that are similar, but not identical to, the previous scaling relations (8.10) and (8.11):

$$H(r, f; ca) = H(r/c, cf; a), \quad (12.12)$$

and

$$h(r, t; ca) = \frac{1}{c} h(r/c, t/c; a), \quad (12.13)$$

where  $c$  is a positive scalar multiplier of the cavity radius  $a$ .

## 12.6 Radiated Energy

The total elastic energy radiated from a spherical cavity may be expressed in terms of the radial displacement applied at  $r = a$ . Starting with equation (9.4), the stress function  $s(t)$  is eliminated in favor of  $u(a, t)$  by utilizing expressions (5.5) and (5.2). Transforming to the frequency-domain gives

$$E(a) = \rho\alpha 4\pi a^2 \int_{-\infty}^{+\infty} |(i2\pi f)U(a, f)|^2 L(a, f) df, \quad (12.14)$$

where

$$L(a, f) \equiv \frac{[f - P_1(a)][f - P_2(a)]}{f[f - Z_1(a)]}. \quad (12.15)$$

$Z_1(a)$  is the zero, and  $P_1(a)$  and  $P_2(a)$  are the poles, of the frequency-domain response function  $G(r, f)$ . [Interestingly, these analytic function roles are reversed in expression (12.15).] All are written in forms emphasizing dependence on the cavity radius  $a$ . If the cavity radius is multiplied by the positive factor  $c$ , then the radiated energy becomes

$$E(ca) = \rho\alpha 4\pi (ca)^2 \int_{-\infty}^{+\infty} |(i2\pi f)U(ca, f)|^2 L(ca, f) df.$$

But equation (12.15) implies  $L(ca, f) = L(a, cf)$ . Thus

$$E(ca) = \frac{1}{c} \rho\alpha 4\pi a^2 \int_{-\infty}^{+\infty} |(i2\pi f)U(ca, f/c)|^2 L(a, f) df. \quad (12.16)$$

If the Fourier spectrum of the cavity wall displacement obeys the scaling rule

$$U(ca, f/c) = c^n U(a, f) \quad (12.17)$$

then (12.16) gives the simple result

$$E(ca) = c^{2n-1} E(a). \quad (12.18)$$

The inverse Fourier transform of (12.17) yields the time-domain scaling condition for the source radial displacement

$$u(ca, t) = c^{n-1} u(a, t/c). \quad (12.19)$$

If exponent  $n = 1$ , then

$$E(ca) = cE(a), \quad u(ca, t) = u(a, t/c).$$

Interestingly, the total radiated energy scales linearly with the cavity radius, in contrast to the analogous situation for an applied pressure or radial stress.

### 12.7 Inverse Impulse Response

Since the impulse response  $h(r, t)$  is minimum delay with respect to the P-wave arrival time  $t = \tau(r)$ , a stable inverse  $h^{-1}(r, t)$  exists that can be used to deconvolve a recorded particle displacement seismogram. From equation (12.4), the convolution of  $h^{-1}(r, t)$  with  $u(r, t)$  yields the displacement waveform applied to the cavity wall:

$$h^{-1}(r, t) * u(r, t) = h^{-1}(r, t) * h(r, t) * u(a, t) = \delta(t) * u(a, t) = u(a, t).$$

The Fourier transform of the inverse impulse response is the reciprocal of the frequency spectrum  $H(r, f)$  in equation (12.3);

$$H^{-1}(r, f) = H(r, f)^{-1} = \left( \frac{r}{a} \right) \left[ \frac{f - Z_1(a)}{f - Z_1(r)} \right] e^{+i2\pi f \tau(r)}. \quad (12.20)$$

Analysis reveals that this expression has the same mathematical form as equation (12.3) above, except that the roles of  $r$  and  $a$  are reversed. Thus, a time-domain expression for the inverse impulse response can be written down by inspection of equation (12.5):

$$h^{-1}(r, t) = \left( \frac{r}{a} \right) \left\{ \delta[t + \tau(r)] - \frac{\alpha}{r} \left( 1 - \frac{r}{a} \right) e^{-\alpha[t + \tau(r)]/r} H[t + \tau(r)] \right\}. \quad (12.21)$$

Convolving  $h^{-1}(r, t)$  with  $u(r, t)$  gives

$$u(a, t) = \left( \frac{r}{a} \right) \left\{ u[r, t + \tau(r)] - \frac{\alpha}{r} \left( 1 - \frac{r}{a} \right) e^{-\alpha[t + \tau(r)]/r} \int_{-\infty}^{t + \tau(r)} u(r, x) e^{+\alpha x/r} dx \right\}. \quad (12.22)$$

## 12.8 ART Representation

An expansion of  $H(r,f)$  in negative powers of frequency  $f$  is convergent for  $|f| > \alpha/2\pi a$ , and yields the asymptotic ray theory representation of the (Fourier transformed) radial particle displacement:

$$U(r, f) = U(a, f) \left[ \sum_{k=0}^{\infty} u_k(r) (i2\pi f)^{-k} \right] e^{-i2\pi f \tau(r)}. \quad (12.23)$$

The amplitude coefficients of the ART expansion are given by

$$u_0(r) = \frac{a}{r}, \quad u_k(r) = \frac{a}{r} \left( 1 - \frac{a}{r} \right) \left( \frac{-\alpha}{a} \right)^k, \quad k = 1, 2, \dots \quad (12.24a,b)$$

The well known *zeroth-order* ART solution is obtained by neglecting terms with  $k > 0$  in the infinite sum of expression (12.22). Thus

$$U(r, f) \approx \left( \frac{a}{r} \right) U(a, f) e^{-i2\pi f \tau(r)}, \quad (12.25a)$$

or in the time-domain

$$u(r, t) \approx \left( \frac{a}{r} \right) u \left( a, t - \frac{r-a}{\alpha} \right). \quad (12.25b)$$

The elastic particle displacement at radius  $r$  is a scaled and delayed version of displacement at radius  $a$ .

## 13.0 NUMERICAL EXAMPLES

**Figure 3** displays radial particle displacement and radial particle velocity responses generated by the step pressure  $p(t) = p_0 H(t)$  within a small spherical cavity of radius  $a = 0.3079$  m ( $\approx 1$  foot). Each trace is labeled with radial distance  $r$  from the center of the source sphere. The elastic wholespace is a hard limestone (called a Solenhofen limestone) with compressional wavespeed  $\alpha = 5354.8$  m/s, shear wavespeed  $\beta = 3091.6$  m/s, and mass density  $\rho = 2670.0$  kg/m<sup>3</sup>. These seismological parameters correspond to Poisson's ratio  $\sigma = 1/4$  and Young's modulus  $Y = 63.8$  GP. Displacement signals, obtained simply by evaluating equation (8.3) above, exhibit a sharp (but continuous) onset at the P-wave arrival times  $\tau(r) = (r - a) / \alpha$ . The onset is followed by approximately a single cycle of damped oscillation, and then the trace asymptotically approaches the static displacement value of equation (8.1). This static offset is clearly a near-field effect; it diminishes rapidly [ $\sim (a/r)^2$ ] with increasing source-receiver distance.

The particle velocity response to a step in pressure is proportional to the displacement impulse response. From equation (7.6):

$$v(r, t) = \frac{\partial u(r, t)}{\partial t} = g(r, t) * \frac{\partial p(t)}{\partial t} = g(r, t) * p_0 \delta(t) = p_0 g(r, t).$$

Thus, velocity traces in figure 3 are obtained simply by evaluating equation (7.5) above. Since each displacement trace has a slope discontinuity at the P-wave arrival time, the corresponding velocity trace possesses a step discontinuity at this same time.

For the Solenhofen limestone parameters, the decay rate  $\alpha_d$  and damped oscillation frequency  $\omega_d$  of the spherical source evaluate to  $\alpha_d = 11,594.3$  radians/second and  $\omega_d = 16,396.7$  radians/second (the latter corresponding to  $f_d = 2609.6$  Hz). For such high damping, the radial particle motion is obviously pulse-like, rather than oscillatory.

The source traction waveform used for the examples illustrated in figures 4 through 8 is a Berlage wavelet (Aldridge, 1990) defined by

$$s(t) = s_0(\omega_s t)^n \exp(-h\omega_s t) \cos(\omega_s t + \varphi_s) H(t).$$

This waveform possesses advantages of causality, continuity, and differentiability. Numerical values of the wavelet parameters are: main frequency  $f_s = \omega_s/2\pi = 30$  Hz; damping factor  $h = 1$ ; time exponent  $n = 3$ ; and initial phase angle  $\varphi_s = -90^\circ$ . The frequency bandwidth of this wavelet (calculated at the 1% level of the Fourier amplitude spectrum) extends from 0 Hz to about 117 Hz.

**Figure 4** depicts pressure signals recorded at horizontal offset distances ranging from 0 m to 500 m from a spherical traction source with radius  $a = 10$  m, and located at the coordinate origin. Pressure receivers are elevated 50 m above the source level. The elastic wholespace is characterized by P-wave speed  $\alpha = 2000$  m/s, S-wave speed  $\beta = 1000$  m/s, and mass density  $\rho = 2000$  kg/m<sup>3</sup>, corresponding to a generic sandstone. Pressure traces are calculated using the frequency-domain analogue of equation (7.12), and then performing a numerical inverse Fourier transformation. **Figure 5** indicates that the source radial stress waveform is recovered by deconvolving each recorded pressure trace, using the inverse (frequency-domain) response function  $G^{-1}(r,f) = G(r,f)^{-1}$  of equation (10.1). As expected, all deconvolved source wavelets have the same onset time (i.e., 0 s), amplitude, and waveshape. The waveform is the Berlage pulse described above.

**Figures 6 and 7** illustrate a similar numerical experiment for the same earth model and recording geometry, but with different source and receiver types. The source consists of a prescribed radial velocity function imposed at the radius  $a = 10$  m. Frequency-domain expressions (12.2) and (12.3) are then used to calculate horizontal (i.e.,  $x$ -component) particle velocity responses at receivers with horizontal offset distances extending from 0 m to 500 m. Note that there is no response at  $x = 0$  m, since the particle motion at this receiver is strictly vertical. Once again, as indicated in figure 7, deconvolving the recorded particle velocity traces [using  $H^{-1}(r,f) = H(r,f)^{-1}$  of equation 12.20)] yields identical source waveforms. Prior to deconvolution, the horizontal component of particle velocity recorded at each receiver must be rotated into the radial direction.

Accurate recovery of the source signature requires knowledge of the elastic parameters of the wholespace and the cavity radius. Interestingly, the deterministic deconvolution operator  $H^{-1}(r,f)$  of equation (12.20) is independent of the S-wave speed  $\beta$  and the mass density  $\rho$ . It depends only on the P-wave speed  $\alpha$  and the cavity radius  $a$ . Hence, an incorrect choice for  $\beta$  and/or  $\rho$  has no influence on source wavelet estimation! **Figure 8** displays source radial velocity waveforms obtained by deconvolving the traces in figure 6 [using  $H^{-1}(r,f)$ ], when the wholespace P-wave speed is incorrectly specified as  $\alpha = 2500$  m/s (i.e., 25% larger than the true value). The wavelets have linear moveout with respect to source-receiver horizontal offset, and amplitude is overestimated by ~10% (compare with figure 7). Source waveforms in **Figure 9** are obtained by erroneously specifying the cavity radius as  $a = 20$  m (i.e., 100% too large). Although the timing, amplitude, and waveshape of the recovered pulses are consistent, all are incorrect.

Finally, it is emphasized that it is not necessary to know the particular type of boundary condition (i.e., radial displacement, velocity, acceleration, traction, etc.) applied to the cavity wall, in order to perform the deterministic trace deconvolution. **Figure 10** illustrates source radial traction waveforms obtained by deconvolving the traces of figure 6 [using  $G^1(r,f) / (i2\pi f)$ ]. Although the horizontal particle velocity traces in figure 6 are originally calculated by applying a radial *velocity* to the cavity wall, the deconvolution procedure accurately recovers the associated source radial *traction* waveform. It is readily established that the positive-going pressure pulse in figure 10 produces the *same* horizontal particle velocity traces (i.e., figure 6) as the oscillatory source radial velocity waveform in figure 7.

## 14.0 CONCLUSION

The closed-form mathematical formulae characterizing elastic waves radiated from a pressurized spherical cavity facilitate rapid and accurate forward modeling. In particular, the solutions developed in this study have already found use in (1) performing order-of-magnitude estimations of seismic responses produced by explosions, and (2) validating purely numerical (i.e., finite-difference or finite-element) solutions of similar problems.

Two obvious limitations of the present solution methodology are:

- 1) The medium surrounding the cavity is considered a homogeneous and isotropic elastic wholespace. If spatial heterogeneity and/or anisotropy is introduced into the earth model, then synthetic seismograms must be calculated by numerical techniques.
- 2) The source boundary condition, and the resulting compressional elastic wavefield, are spherically symmetric. However, this particular limitation is not fundamental, and may be relaxed. Figure 11 depicts a spherical cavity embedded within a homogeneous and isotropic elastic wholespace, and subject to an arbitrary boundary condition at the cavity wall. The boundary condition entails a prescribed displacement, velocity, acceleration, or traction function at  $r = a$ , which may vary in magnitude, direction, and/or waveform over the spherical interface. In this situation, non-symmetrical compressional (P) and shear (S) waves will be generated. The particle displacement vector  $\mathbf{u}(\mathbf{r},t)$  has radial and tangential components which depend on the two angular coordinates  $\theta$  and  $\phi$ , in addition to the radius  $r$ . Although this situation is considerably more complicated, the problem is still amenable to mathematical solution. The Fourier transformed elastic wavefield may be obtained as an infinite series involving spherical Hankel functions and spherical vectors (a vector-valued generalization of spherical harmonics; see Korneev and Johnson, 1993). Although this solution would allow computation of synthetic seismograms generated by asymmetrical explosions, the corresponding inverse problem (i.e., source signature estimation) is not particularly well defined.

## 15.0 REFERENCES

- Aldridge, D.F., 1990, The Berlage wavelet: *Geophysics*, **55**, 1508-1511.
- Ben-Menahem, A., and Singh, S.J., 1981, *Seismic waves and sources*: Springer-Verlag.
- Blake, Jr., F.G., 1952, Spherical wave propagation in solid media: *Journal of the Acoustical Society of America*, **24**, 211-215.
- Bracewell, R., 1965, *The Fourier transform and its applications*: McGraw-Hill Book Company.
- Denny, M.D., and Johnson, L.R., 1991, The explosion seismic source function: models and scaling laws revisited, *in* *Explosion source phenomenology*, edited by Taylor, S.R, Patton, H.J., and Richards, P.G.: Geophysical Monograph 65, American Geophysical Union.
- Duvall, W.I., 1953, Strain-wave shapes in rock near explosions: *Geophysics*, **18**, 310-323.
- Eringen, A.C., 1957, Elasto-dynamic problem concerning the spherical cavity: *Quarterly Journal of Mechanics and Applied Mathematics*, **10**, 257-270.
- Eringen, A.C., and Suhubi, E.S., 1975, *Elastodynamics*, volume 2, linear theory: Academic Press.
- Goldsmith, W., and Allen, W.A., 1955, Graphical representation of the spherical propagation of explosive pulses in elastic media: *Journal of the Acoustical Society of America*, **27**, 47-55.
- Graff, K.F., 1975, *Wave motion in elastic solids*: Ohio State University Press.
- Gurvich, I.I., 1965, The theory of spherical radiators of seismic waves: *Physics of the Solid Earth*, no volume number, 684-689 (English translation edition).
- Jeffreys, H., 1931, On the cause of oscillatory movement in seismograms: *Monthly Notices of the Royal Astronomical Society, Geophysical Supplement*, **2**, 407-416.
- Kawasumi, H., and Yosiyama, R., 1935, On an elastic wave animated by the potential energy of initial strain: *Bulletin of the Earthquake Research Institute*, **13**, 496-503.
- Korneev, V.A., and Johnson, L.R., 1993, Scattering of elastic waves by a spherical inclusion – I. Theory and numerical results: *Geophysical Journal International*, **115**, 230-250.
- Kramer, F.S., Peterson, R.A., and Walter, W.C., 1968, *Seismic energy sources, 1968 handbook*: Bendix-United Geophysical Corporation.
- Latter, A.L., Martinelli, E.A., and Teller, E., 1959, Seismic scaling law for underground explosions: *Physics of Fluids*, **2**, 280-282.
- Miklowitz, J., 1978, *The theory of elastic waves and waveguides*: North-Holland Publishing Company.
- Peet, W.E., 1960, A shock wave theory for the generation of the seismic signal around a spherical shot hole: *Geophysical Prospecting*, **8**, 509-533.

Sezawa, K., 1935, Elastic waves produced by applying static force to a body or by releasing it from a body: *Bulletin of the Earthquake Research Institute*, **13**, 740-749.

Sezawa, K., and Kanai, K., 1936, Elastic waves formed by local stress changes of different rapidities: *Bulletin of the Earthquake Research Institute*, **14**, 10-17.

Sharpe, J.A., 1942, The production of elastic waves by explosion pressures. I. Theory and empirical field observations: *Geophysics*, **7**, 144-154.

Wylde, H.W., 1976, *Mathematical methods for physics*: W.A. Benjamin Inc.

Ziolkowski, A., Lerwill, W.E., March, D.W., and Peardon, L.G., 1980, Wavelet deconvolution using a source scaling law: *Geophysical Prospecting*, **28**, 872-901.

Ziolkowski, A., 1993, Determination of the signature of a dynamite source using source scaling, part 1: theory: *Geophysics*, **58**, 1174-1182.

Ziolkowski, A., and Bokhorst, K., 1993, Determination of the signature of a dynamite source using source scaling, part 2: experiment: *Geophysics*, **58**, 1183-1194.

## 16.0 FIGURES

**Figure 1:** Spherically symmetric seismic source model.

**Figure 2:** Definition of equivalent linear elastic radius.

**Figure 3:** Radial particle displacement and velocity responses to a step pressure  $p(t) = p_0 H(t)$  applied to spherical cavity wall at  $a = 0.3079$  m.

**Figure 4:** Pressure traces generated by a spherical cavity source with prescribed radial traction imposed at  $a = 10$  m.

**Figure 5:** Source radial traction waveforms obtained by deconvolving the pressure traces displayed in figure 4. Each recovered waveform is a Berlage wavelet.

**Figure 6:** Horizontal ( $x$ -component) particle velocity traces generated by a spherical cavity source with prescribed radial velocity imposed at  $a = 10$  m.

**Figure 7:** Source radial velocity waveforms obtained by deconvolving the horizontal ( $x$ -component) particle velocity traces displayed in figure 6.

**Figure 8:** Estimated source radial velocity waveforms obtained by deconvolving the horizontal ( $x$ -component) particle velocity traces displayed in figure 6. P-wave speed  $\alpha$  specified 25% larger than correct value.

**Figure 9:** Estimated source radial velocity waveforms obtained by deconvolving the horizontal ( $x$ -component) particle velocity traces displayed in figure 6. Cavity radius specified 100% larger than correct value.

**Figure 10:** Source radial traction waveforms obtained by deconvolving the horizontal ( $x$ -component) particle velocity traces displayed in figure 6.

**Figure 11:** General spherical source model.

# Spherical Seismic Source

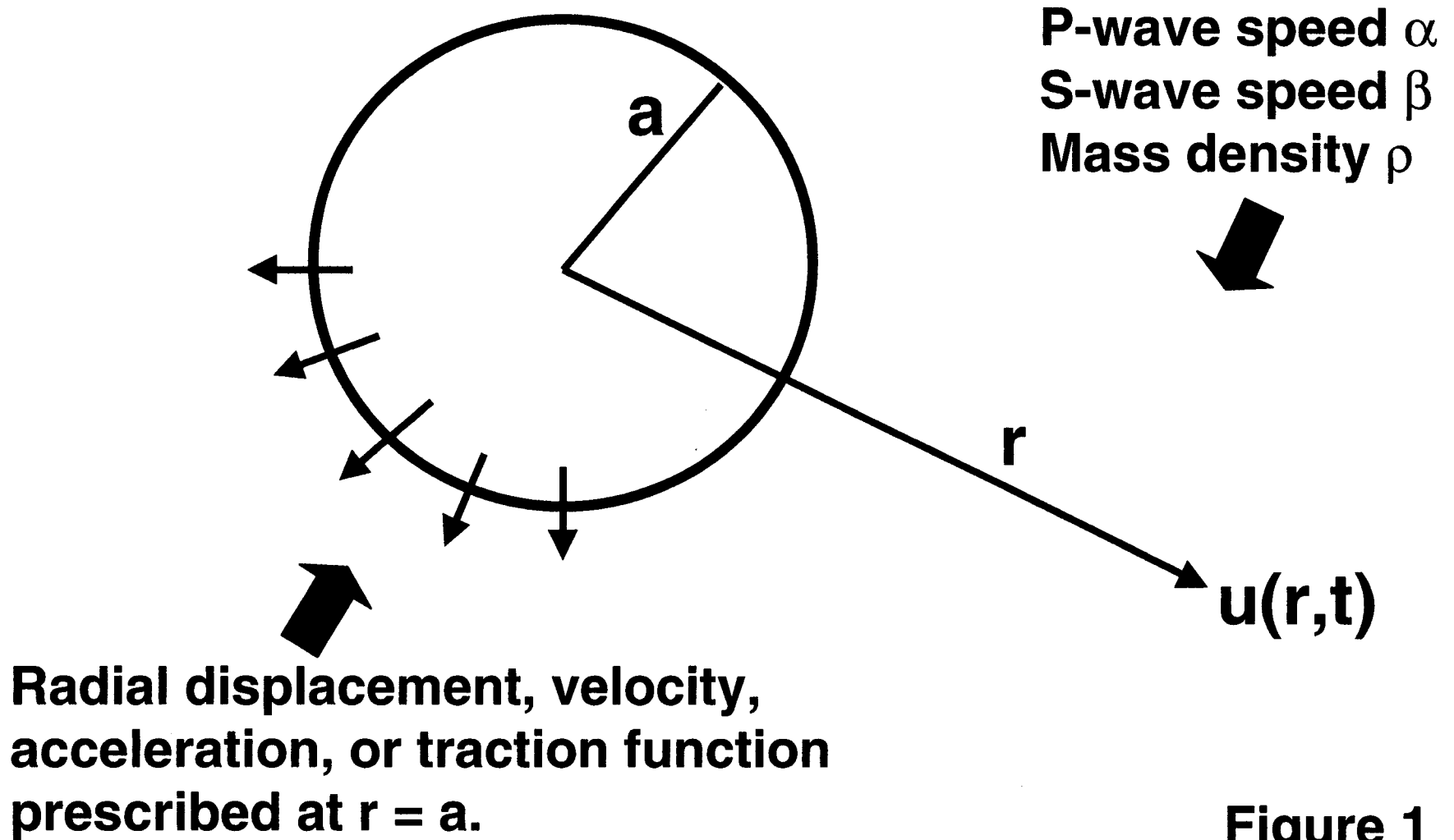


Figure 1

# Equivalent Elastic Radius

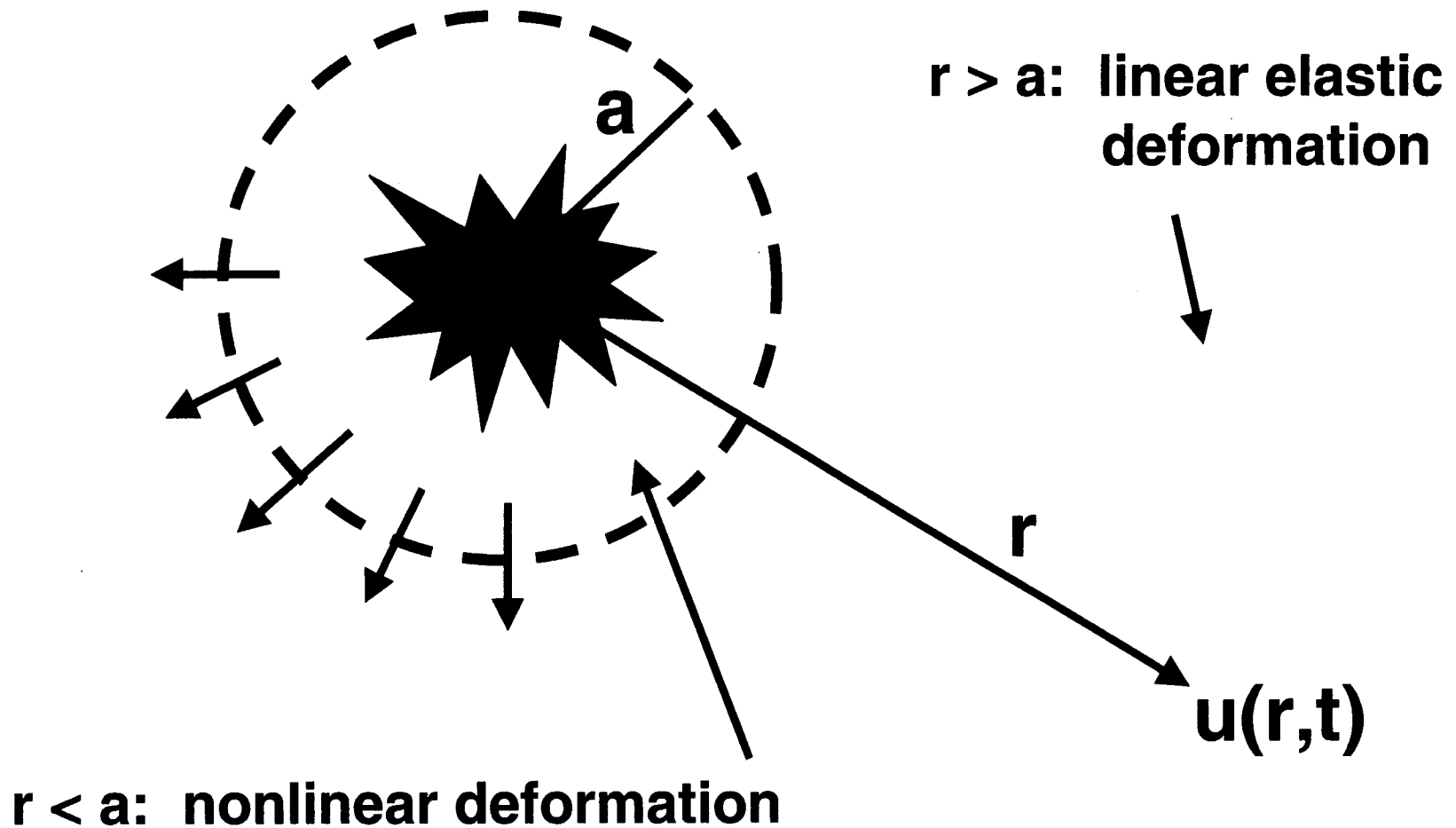
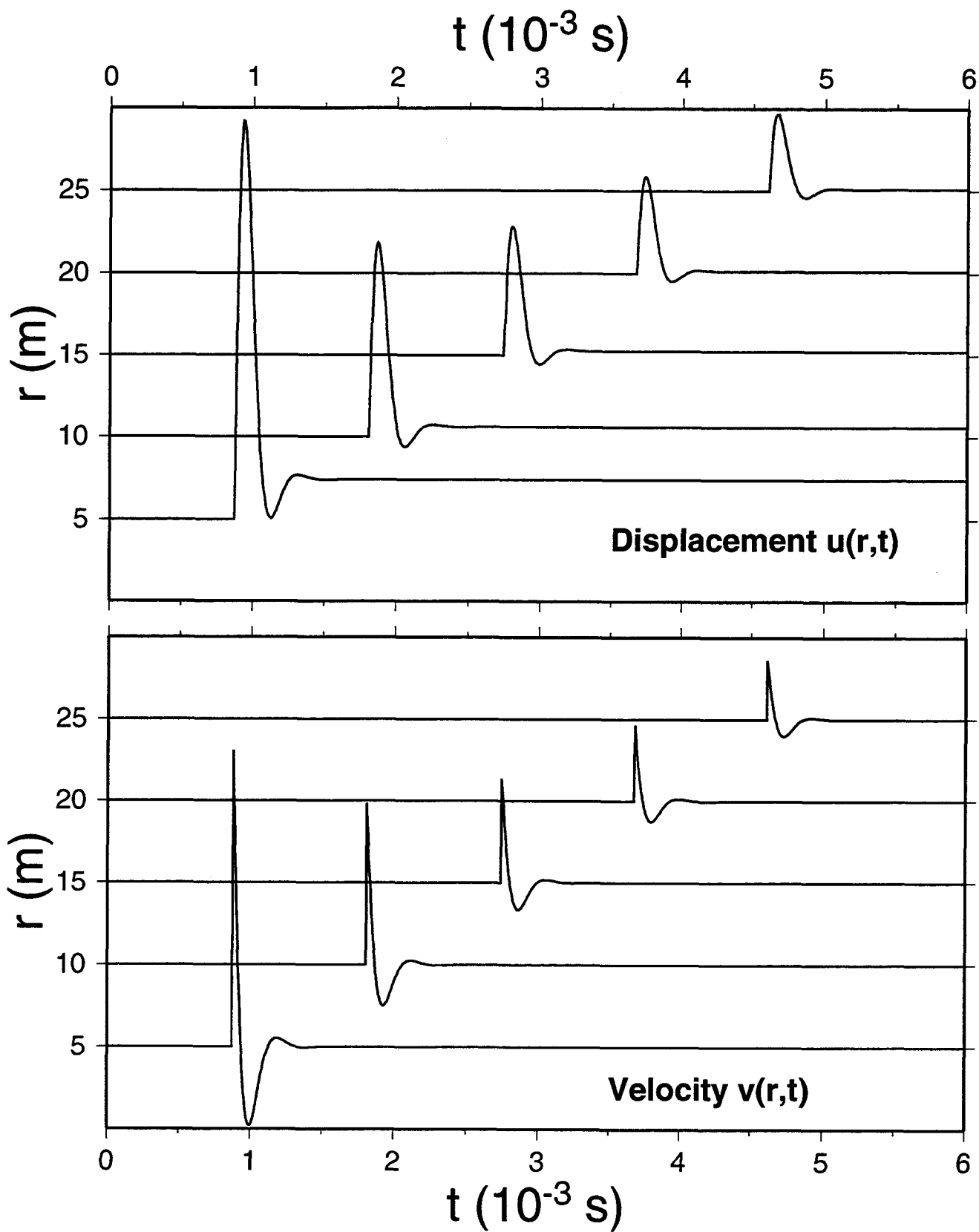
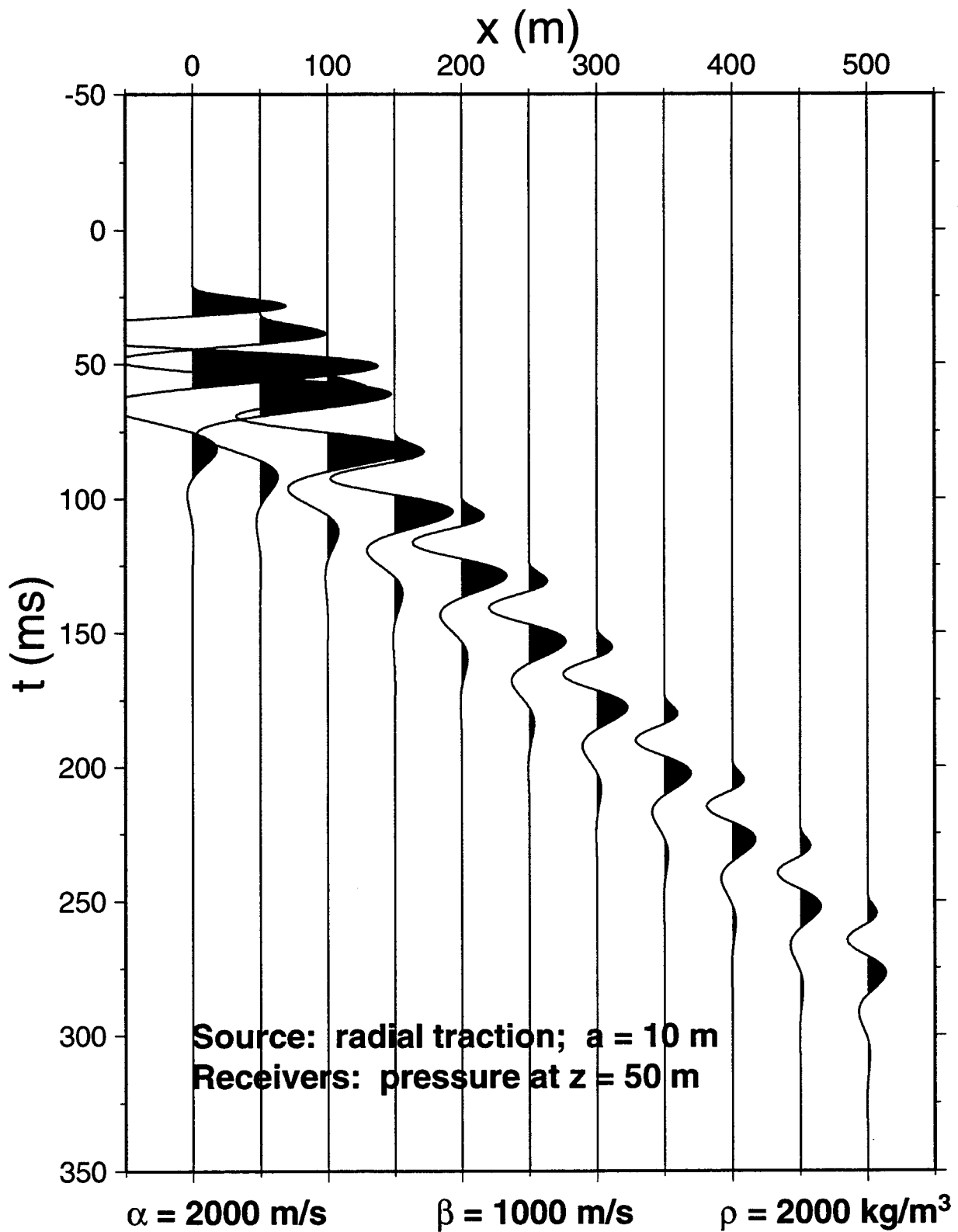


Figure 2



**Figure 3**



**Figure 4**

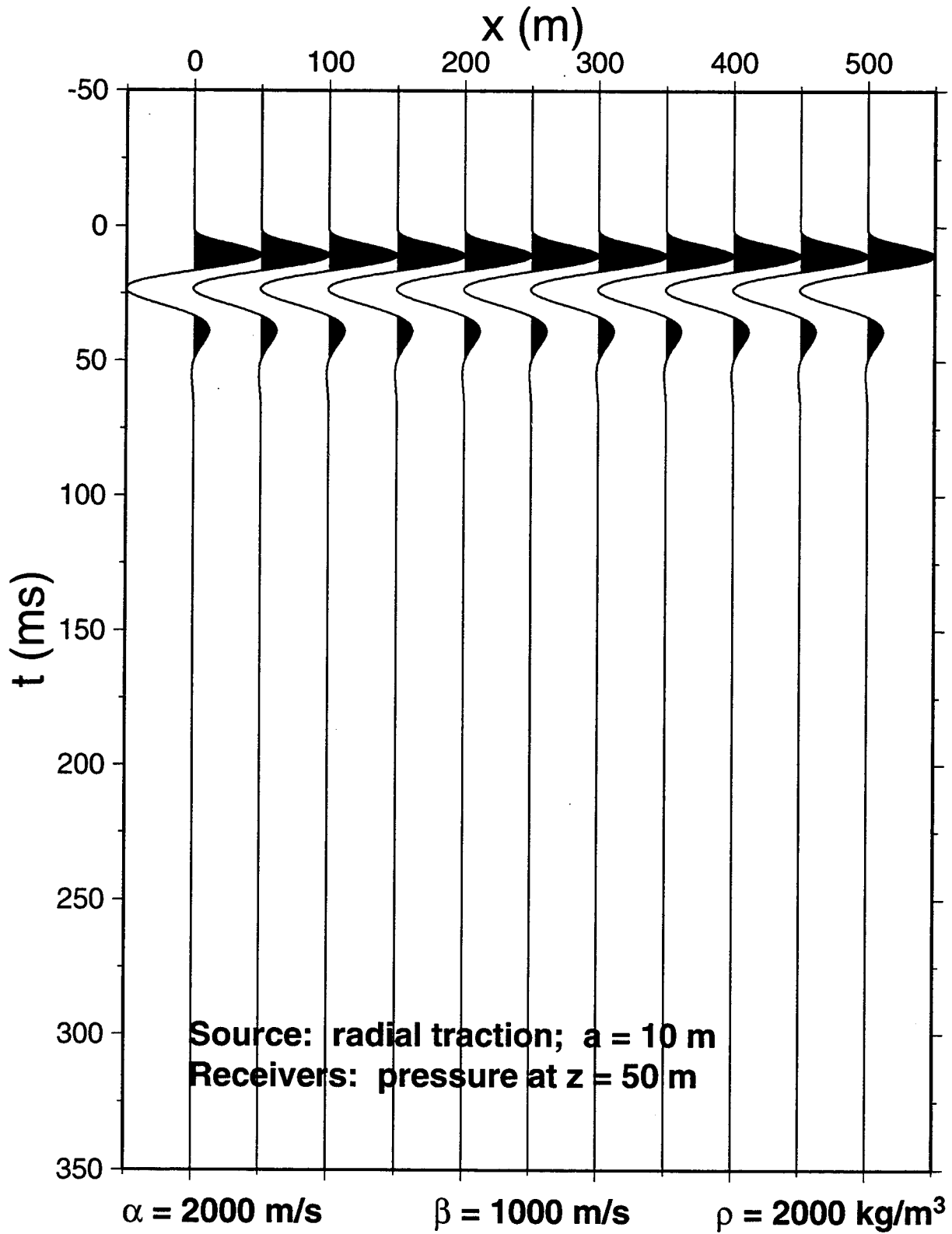


**Figure 5**

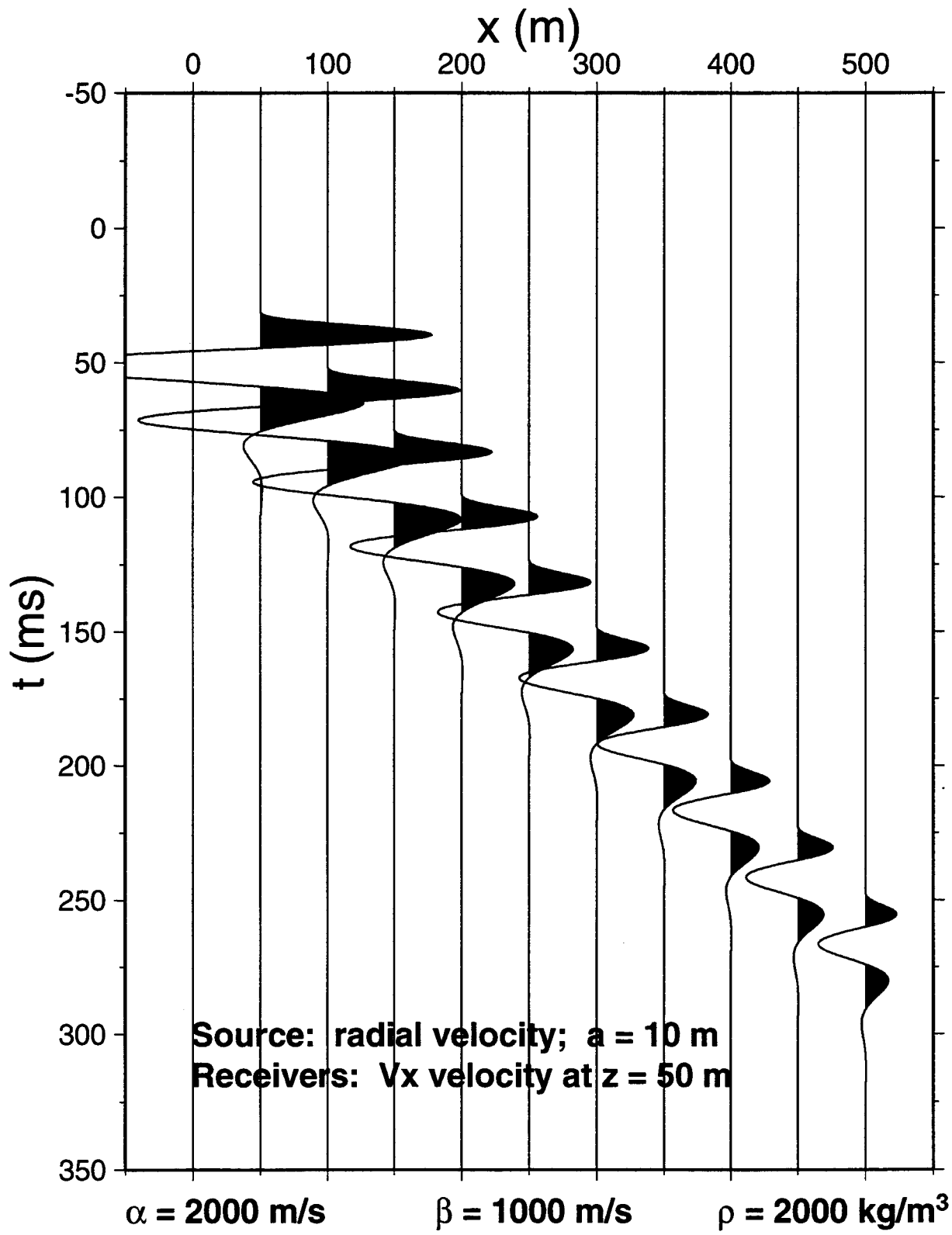


**Figure 6**

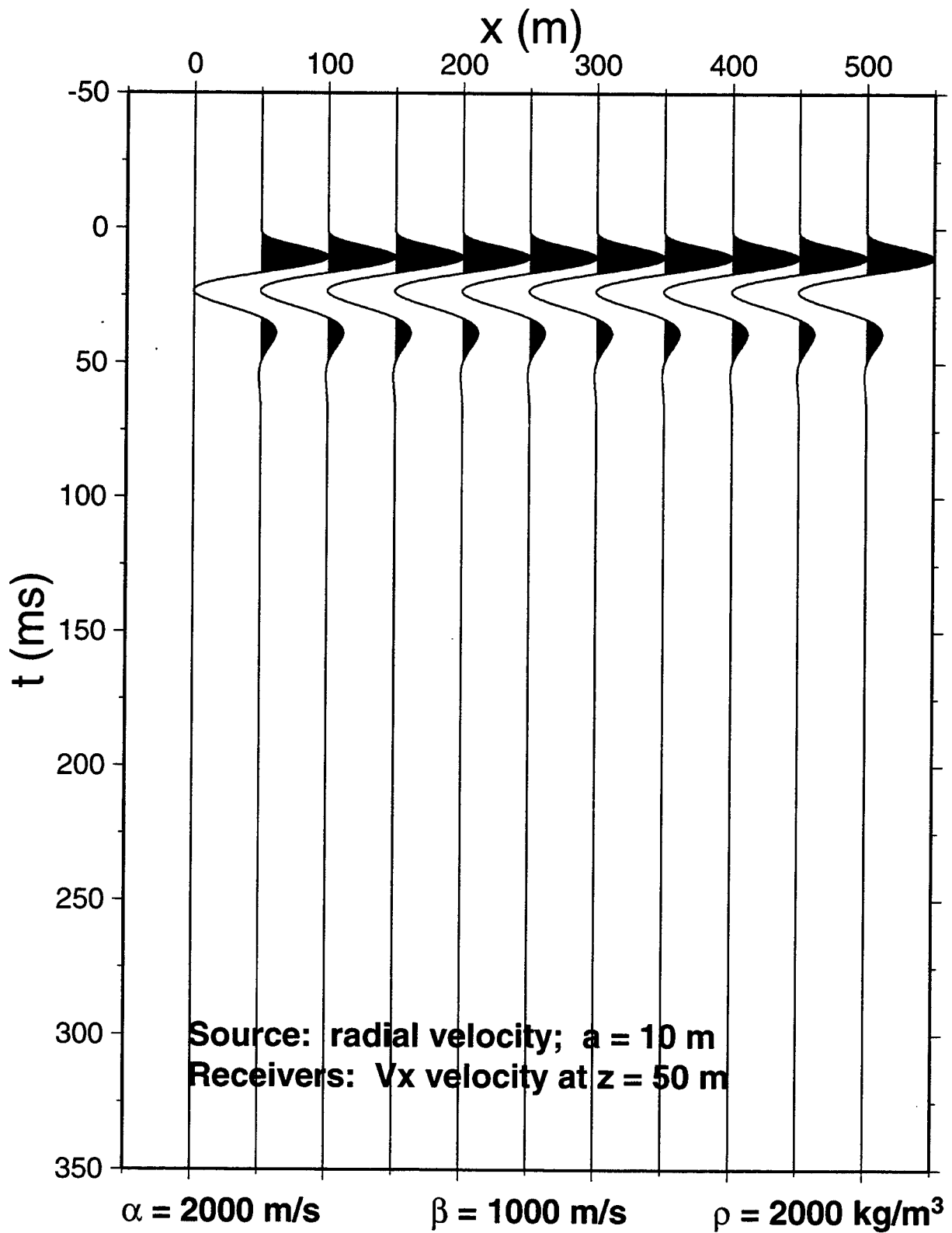


**Figure 7**

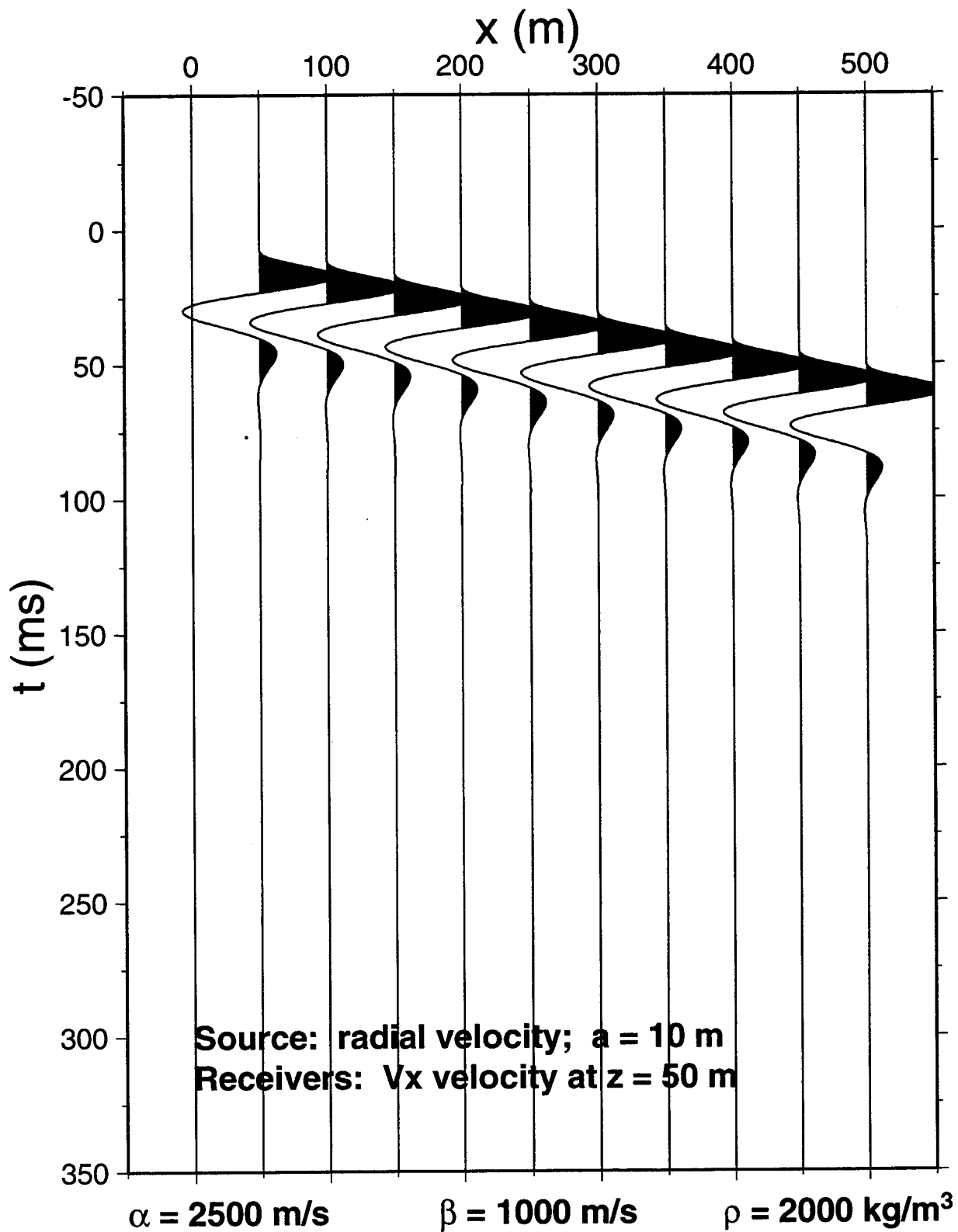


**Figure 8**

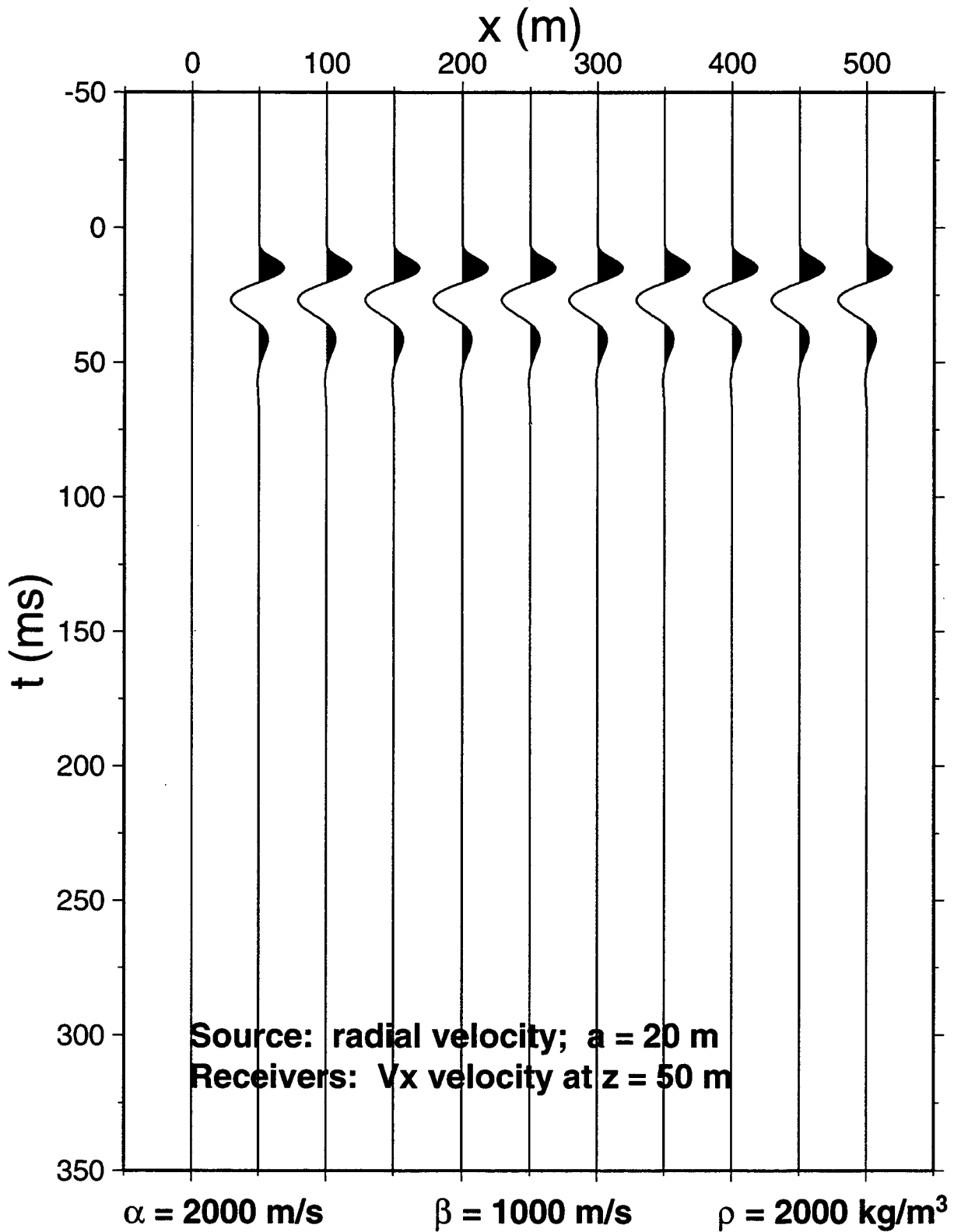


**Figure 9**

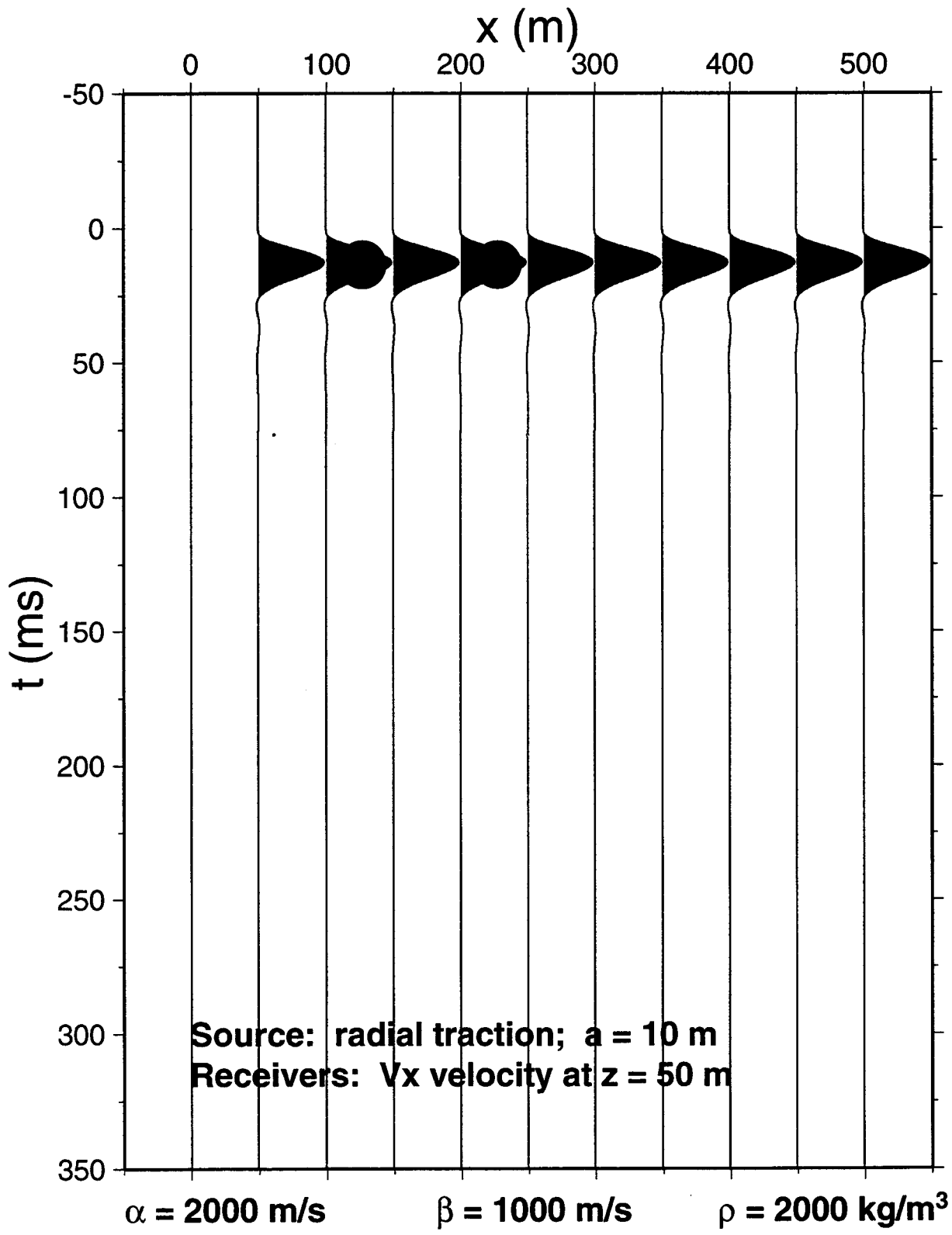


**Figure 10**

# General Spherical Source

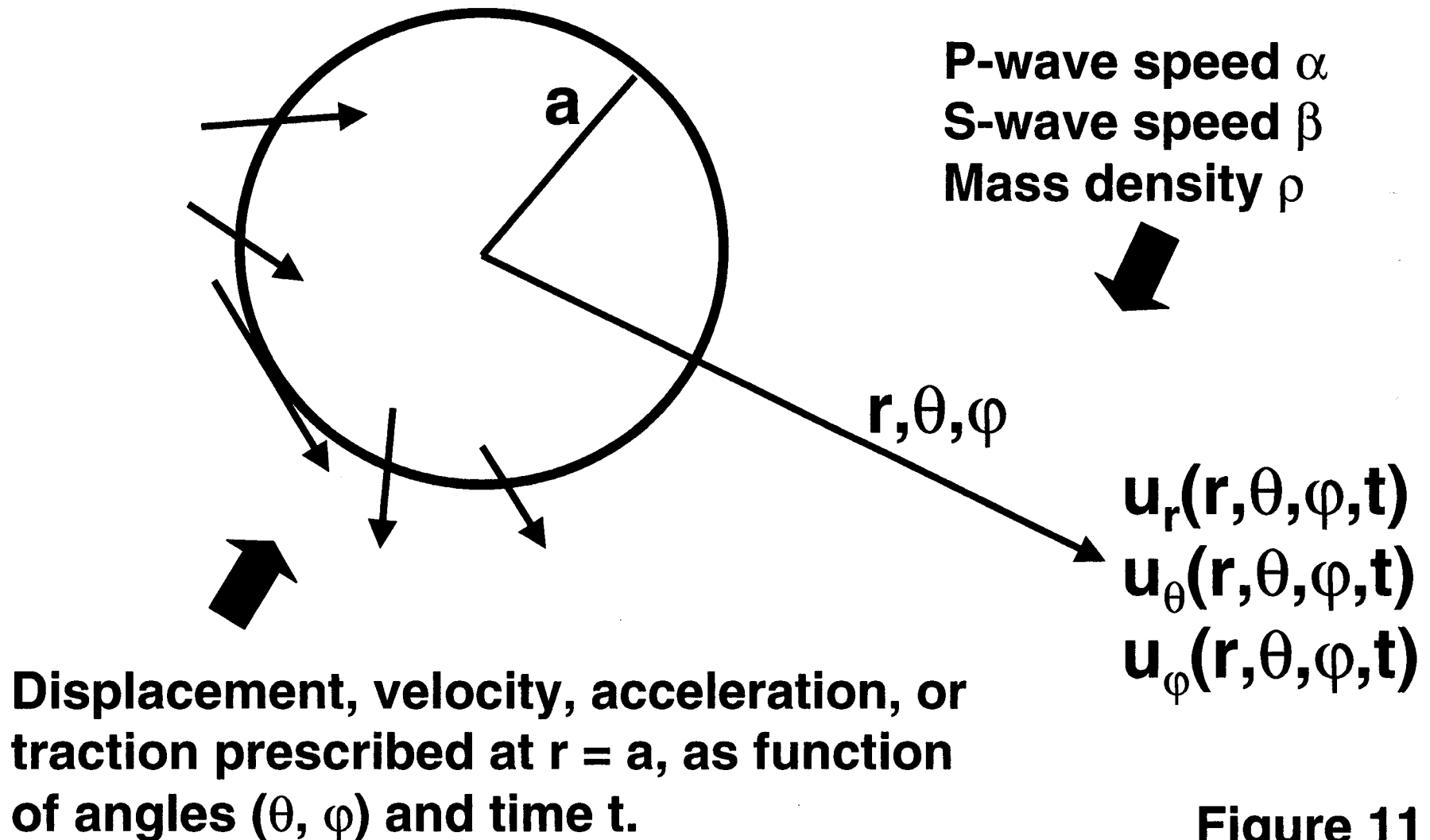


Figure 11

## DISTRIBUTION LIST

1 MS 0329 Gerard E. Sleafte (02614)  
1 MS 0329 Darren A. Hoke (02614)  
1 MS 0612 Review and Approval Desk (09612)  
25 MS 0750 David F. Aldridge (06116)  
1 MS 0750 Lewis C. Bartel (06116)  
1 MS 0750 David J. Borns (06116)  
1 MS 0750 Gregory J. Elbring (06116)  
1 MS 0750 Bruce P. Engler (06116)  
1 MS 0750 Kyoung-Tae Kim (06116)  
1 MS 0750 Gregory A. Newman (06116)  
1 MS 0750 Neill P. Symons (06116)  
1 MS 0750 Chester J. Weiss (06116)  
1 MS 0750 Marianne C. Walck (06116)  
1 MS 0750 Norman R. Warpinski (06116)  
1 MS 0835 Timothy F. Walsh (09142)  
1 MS 0847 Jose G. Arguello, Jr. (09126)  
1 MS 0847 John F. Holland (09126)  
1 MS 0859 Mark D. Ladd (15351)  
1 MS 0859 K. Terry Stalker (15351)  
1 MS 0975 Eric P. Chael (05736)  
1 MS 1033 Douglas S. Drumheller (06211)  
1 MS 1080 Jeffrey L. Dohner (01769)  
1 MS 1138 Christopher J. Young (06533)  
1 MS 1168 H. Douglas Garbin (01612)  
1 MS 1168 Robert E. Abbott (01612)  
2 MS 0899 Technical Library (09616)  
For DOE/OSTI  
1 MS 9018 Central Technical Files (08945-1)